Published in final edited form as:

Curr Biol. 2021 February 08; 31(3): 502–514.e7. doi:10.1016/j.cub.2020.10.061.

CK2 Inhibits TIMELESS Nuclear Export and Modulates CLOCK Transcriptional Activity to Regulate Circadian Rhythms

Yao D. Cai[1], **Yongbo Xue**[2], **Cindy C. Truong**[1], **Jose Del Carmen-Li**[1], **Christopher Ochoa**[1], **Jens T. Vanselow**[3], **Katherine A. Murphy**[1], **Ying H. Li**[1], **Xianhui Liu**[1], **Ben L. Kunimoto**[1], **Haiyan Zheng**[4], **Caifeng Zhao**[4], **Yong Zhang**[2], **Andreas Schlosser**[3], **Joanna C. Chiu**[1,5,*]

[1]Department of Entomology and Nematology, College of Agricultural and Environmental Sciences, University of California, Davis, One Shields Avenue, Davis, CA 95616, USA

[2]Department of Biology, University of Nevada, Reno, NV 89557, USA

[3]Rudolf Virchow Center for Experimental Biomedicine, University of Wurzburg, Wurzburg, Germany

[4]Biological Mass Spectrometry Facility, Robert Wood Johnson Medical School and Rutgers, the State University of New Jersey, Piscataway, NJ 08854, USA

[5]Lead Contact

SUMMARY

Circadian clocks orchestrate daily rhythms in organismal physiology and behavior to promote optimal performance and fitness. In *Drosophila,* key pacemaker proteins PERIOD (PER) and TIMELESS (TIM) are progressively phosphorylated to perform phase-specific functions. Whereas PER phosphorylation has been extensively studied, systematic analysis of site-specific TIM phosphorylation is lacking. Here, we identified phosphorylation sites of PER-bound TIM by mass spectrometry, given the importance of TIM as a modulator of PER function in the pacemaker. Among the 12 TIM phosphorylation sites we identified, at least two of them are critical for circadian timekeeping as mutants expressing non-phosphorylatable mutations exhibit altered behavioral rhythms. In particular, we observed that CK2-dependent phosphorylation of TIM(S1404) promotes nuclear accumulation of PER-TIM heterodimers by inhibiting the interaction of TIM and nuclear export component, Exportin 1 (XPO1). We propose that proper level of nuclear PER-TIM accumulation is necessary to facilitate kinase recruitment for the regulation of daily phosphorylation rhythm and phase-specific transcriptional activity of CLOCK (CLK). Our results highlight the contribution of phosphorylation-dependent nuclear export of

*Correspondence: jcchiu@ucdavis.edu.

AUTHOR CONTRIBUTIONS

J.C.C., Y.D.C., and A.S. designed research; Y.D.C., Y.X., C.C.T., J.D.C.-L., C.O., K.A.M., Y.H.L., B.L.K., J.T.V., H.Z., and C.Z. performed research and analyzed data; Y.D.C., J.C.C., Y.X., Y.Z., and A.S. contributed to critical interpretation of the data; X.L. and K.A.M. generated reagents; and Y.D.C., A.S., and J.C.C. wrote the paper.

SUPPLEMENTAL INFORMATION

Supplemental Information can be found online athttps://doi.org/10.1016/j.cub.2020.10.061.

DECLARATION OF INTERESTS

The authors declare no competing interests.

PER-TIM heterodimers to the maintenance of circadian periodicity and identify a new mechanism by which the negative elements of the circadian clock (PER-TIM) regulate the positive elements (CLK-CYC). Finally, because the molecular phenotype of *tim*(S1404A) non-phosphorylatable mutant exhibits remarkable similarity to that of a mutation in human *timeless* that underlies familial advanced sleep phase syndrome (FASPS), our results revealed an unexpected parallel between the functions of *Drosophila* and human TIM and may provide new insights into the molecular mechanisms underlying human FASPS.

Graphical Abstract

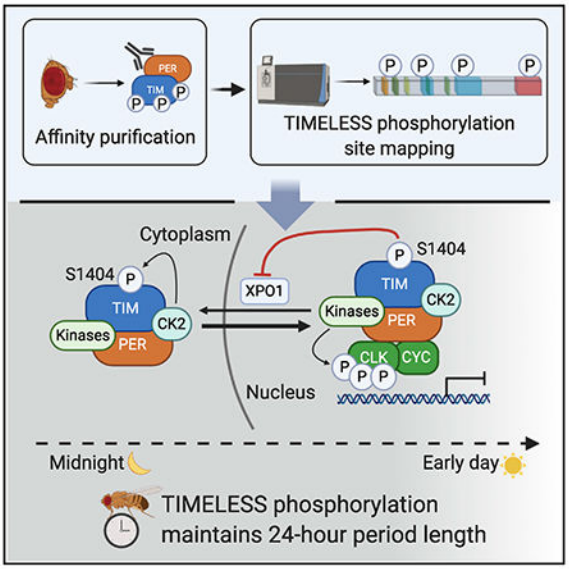

In Brief

Organisms in all domains of life exhibit circadian rhythms. Cai et al. reveal that phosphorylation of TIMELESS modulates kinase accessibility to CLOCK in the nucleus. This mechanism is important in controlling daily phosphorylation rhythm of CLOCK, which is critical for its function as a key regulator of circadian rhythms.

INTRODUCTION

Circadian rhythms have been observed in all domains of life and are driven by a network of cellular molecular clocks in animals.[1–3] These molecular clocks are entrained by environmental time cues, such as light-dark (LD) cycles, to control daily rhythms in physiology and behavior. One conserved feature of molecular clocks within the animal kingdom is their reliance on key clock proteins that are organized in transcriptional translational feedback loops (TTFLs).[3,4] In *Drosophila,* these key pacemaker proteins are the positive elements, CLOCK (CLK) and CYCLE (CYC), and the negative elements, PERIOD (PER) and TIMELESS (TIM). During the day, CLK-CYC heterodimers activate the transcription of *per, tim,* and other clock-controlled genes (ccgs).[5] The accumulation of PER and TIM proteins is delayed by a number of post-transcriptional and post-translational mechanisms[6–10] until early night, when PER and TIM attain high enough levels to form

heterodimeric complexes in the cytoplasm prior to nuclear entry.[11,12] Nuclear PER, likely still in complex with TIM, promotes the repression of the circadian transcriptome by inhibiting CLK-CYC transcriptional activity and removing them from clock genes before its degradation in the late night and early day.[13–17]

Although TIM itself cannot repress CLK-CYC transcriptional activity, it is essential to the molecular clock because it maintains rhythmic PER protein expression.[18–20] Constitutive cytoplasmic PER in *tim null* mutants[21] as well as in *tim* mutants with defective nuclear entry[22,23] abolishes rhythms in the molecular clock and consequently dampens behavioral rhythms. An early study suggested that TIM physically associates to the PER cytoplasmic localization domain (CLD) and thus blocks cytoplasmic retention.[11] A subsequent study showed that TIM actively facilitates PER nuclear entry by acting as the primary cargo of importin α1 (IMPα1)-dependent nuclear import mechanisms and cotransport PER into the nucleus.[12] Finally, TIM is suggested to counteract the effect of DOUBLETIME (DBT) kinases in preventing PER nuclear entry.[20] Taken together, TIM is proposed to promote the nuclear entry of PER.

Phosphorylation has also been implicated in regulating PER-TIM nuclear entry. The function of casein kinase 1α (CK1α), casein kinase 2 (CK2), SHAGGY (SGG), and DBT have been investigated in this context. DBT has been observed to phosphorylate PER and prevent nuclear translocation.[20] This regulatory step has recently been shown to be antagonized by CK1α-dependent phosphorylation of either PER or DBT.[24] The role of CK2 and SGG in regulating PER-TIM subcellular localization has received relatively more attention. Early studies suggest that SGG and CK2 phosphorylate both PER and TIM to promote nuclear translocation.[25–27] Subsequent studies indicate that PER may be the primary target of CK2 and SGG to control subcellular localization.[28,29] However, more recent studies indicate that perhaps CK2 regulates nuclear entry of PER-TIM by phosphorylating TIM.[30,31] In addition to kinases, protein phosphatase 1 (PP1) and protein phosphatase 2A (PP2A) have also been shown to influence PER-TIM nuclear accumulation.[32,33]

In addition to its role in facilitating PER nuclear entry, TIM has been observed to mediate light resetting and circadian entrainment because of its light-induced degradation.[34,35] Upon light exposure, the blue light photoreceptor CRYPTOCHROME (CRY) undergoes a conformational change and binds to TIM.[36,37] The E3 ubiquitin ligase JETLAG (JET) then collaborates with CRY to promote rapid proteasomal degradation of TIM.[36,38,39] Phosphorylation of yet uncharacterized tyrosine residues has been proposed to be required for degradation.[40] Finally, light-induced TIM degradation further promotes PER turnover, which functions to reset and entrain the molecular clock.[35]

Significant progress has been made in examining the function of site-specific PER phosphorylation, enabling in-depth mechanistic understanding of post-translational regulation of PER subcellular localization, repressor activity, and degradation to generate a 24-h rhythm.[28,29,41–45] On the other hand, the relative dearth of studies that characterize site-specific functions of TIM phosphorylation[22,31,46] remains a significant obstacle to fully understand the regulation of circadian rhythms via post-translational regulation of TIM and

PER-TIM complexes. In this study, we used mass spectrometry proteomics to identify phosphorylation sites of PER-bound TIM proteins purified from *Drosophila* heads. We found that loss of phosphorylation at some of these TIM residues resulted in altered circadian behavioral rhythms. In particular, impaired CK2-dependent phosphorylation at TIM(S1404) resulted in an ~1.7-h period-shortening phenotype. By analyzing the molecular clock of non-phosphorylatable *tim*(S1404A) and phosphomimetic *tim*(S1404D) mutants, we provide evidence supporting the importance of TIM(S1404) phosphorylation in promoting TIM nuclear retention by reducing its interaction with exportin 1 (XPO1), an important component of the nuclear export machinery. Interestingly, decreased nuclear localization of TIM in *tim*(S1404A) mutant flies not only reduces the abundance of nuclear PER and TIM proteins but also dampens the daily rhythms in CLK phosphorylation. We reasoned this is caused by changes in the abundance of kinases recruited by the PER-TIM complexes to phosphorylate CLK. Consequently, this leads to phase advance of CLK occupancy rhythms at circadian promoters, which manifests into shortening of molecular and behavioral rhythms. Based upon these findings, we propose a model describing the mechanism by which CK2-dependent TIM(S1404) phosphorylation regulates PER-TIM nuclear accumulation and CLK-CYC activity to regulate circadian rhythms.

RESULTS

Mass Spectrometry Analysis Identifies TIM Phosphorylation Sites in PER-TIM Heterodimers

Comprehensive mapping of TIM phosphorylated sites has not been performed despite previous studies indicating that phosphorylation is important for the phase-specific regulation of TIM function.[25–27,31,40,46] This hinders further understanding of the mechanisms by which site-specific TIM phosphorylation regulates the molecular clock. Because TIM interacts with PER to achieve its role in circadian timekeeping, we aimed to identify phosphorylated TIM residues in the PER-TIM heterodimeric complex. Previously, our group identified PER phosphorylation sites by purifying PER from fly heads followed by mass spectrometry (MS) analysis.[47] Proteins extracted from tissues of *wper*^{0}; *p*{3XFLAG-*per*(WT)} flies were subjected to FLAG affinity purification prior to MS analysis. We observed that TIM was copurified with PER at ZT1 (ZT is defined as Zeitgeber Time), ZT3, ZT12, ZT16, ZT20, and ZT23.5 and leveraged this opportunity to identify PER-bound TIM phosphorylation sites. The MS data from multiple time points were pooled to identify TIM phosphorylation sites qualitatively. We expect that some of these phosphorylation events may be critical in regulating PER-TIM interactions and the function of PER-TIM heterodimer in the molecular clock.

We identified 12 TIM phosphorylation sites, some of which are located in previously characterized functional domains (Figure 1A; Table S1). These include S568, which is in PER binding domain 1 (PER BD1) and the NLS (nuclear localization signal);[11] S891 in PER binding domain 2 (PER BD 2);[11] and S1389, S1393, S1396, and S1404 in the cytoplasmic localization domain (CLD).[11] Based on the location of these phosphorylation sites, we reasoned that they may regulate the subcellular localization and phase-specific functions of PER-TIM heterodimers. We also identified a number of other phosphorylated

residues that are located in regions of TIM proteins without characterized functions. Finally, although not the central focus of this study, we determined that TIM, like PER and CLK,[47–49] is O-GlcNAcylated at multiple residues (Table S1).

Transgenic Flies Expressing Non-phosphorylatable TIM Variants Display Altered Locomotor Activity Rhythms

To determine whether the TIM phosphorylation sites we identified play important roles in circadian timekeeping, we generated transgenic fly lines each expressing one or a cluster of non-phosphorylatable S/T to A mutations. We prioritized our efforts by focusing on sites with high MS probability score and/or those located in characterized functional domains. *p*{*tim*(X)-3XFLAG-6XHIS} transgenes (X represents the S/T to A TIM mutation or wild-type [WT] TIM) were crossed into tim^0 genetic background[53] such that only transgenic *tim* was expressed. First, we evaluated daily locomotor activity rhythms of *tim* transgenic flies as activity rhythm is a reliable behavioral output of the *Drosophila* circadian clock.[54] Flies were entrained for 3 days in cycles of 12 h light and 12 h darkness (herein referred as LD cycles) followed by 7 days in constant darkness (DD) to monitor free-running rhythm. We observed that homozygous *tim*(WT) flies exhibited behavioral rhythm with an ~24-h period, indicating that the arrhythmic tim^0 mutation was rescued by the *tim*(WT) transgene (Figures 1B, S1A, and S1B; Table S2). Rescue of tim^0 mutants with various *tim* transgenes over the years have yielded variable results. Although the behavioral rhythmicity of *tim*(WT) in this experiment (43.6%) is somewhat lower than the extent of tim^0 rescue observed in some previous studies (e.g., Top et al.[31] and Ousley et al.[50]), it is notably higher than rescue of tim^0 flies by driving expression of *tim* cDNA using *tim*-Gal4.[22,54] Among the transgenic lines expressing TIM variants, *tim*(S1404A) was the only genotype that exhibited a clear period-shortening phenotype (~1.7 h shorter), although *tim*(S568A) flies were notably more arrhythmic when compared to *tim*(WT).

Among the two phosphorylation sites that resulted in changes in behavioral rhythms when mutated, we decided to proceed first with the functional characterization of TIM(S1404) as it is (1) highly conserved in animals (Figures S2A and S2B); (2) predicted to be phosphorylated by CK2, a known clock kinase; (3) also phosphorylated in the monarch butterfly TIM protein as determined by MS analysis (Figure S2C); and (4) located within TIM CLD (Figure 1A). For this reason, we generated an additional transgenic fly line expressing a phosphomimetic S1404D TIM variant to complement the analysis of *tim*(S1404A) mutants. Interestingly, *tim*(S1404D) flies also exhibited shortened period, similar to what was observed in *tim*(S1404A) flies (Figures 1B and S1B; Table S2). Although it is logical to assume that non-phosphorylatable and phosphomimetic mutations should result in opposite phenotypes (e.g., Top et al.[31] and Chiu et al.[41]), that is often not the case, as observed in previous phosphorylation studies (e.g., Lin et al.,[28] Chiu et al.,[42] and Top et al.[45]). Furthermore, although both *tim*(S1404A) and *tim*(S1404D) mutants exhibit period shortening at the behavioral level, the underlying molecular mechanisms that underlie their phenotypes may differ.

TIM(S1404) Phosphorylation Promotes TIM Nuclear Accumulation

Because TIM S1404 residue is located in the CLD, we reasoned that S1404 phosphorylation may regulate TIM nuclear accumulation. To test our hypothesis, we monitored subcellular localization of TIM in *tim*(WT), *tim*(S1404A), and *tim*(S1404D) adult brain clock neurons from early to late night using whole-mount immunocytochemistry. These experiments were performed using flies entrained in LD cycles to preclude phase differences between the genotypes that are caused by alterations in period length. Costaining of TIM with pigment-dispersing factor (PDF) enabled the identification of PDF+ clock neurons (small lateral ventral neurons [sLN_vs] and large lateral ventral neurons [ILN_vs]), and demarcation of nuclear versus cytoplasmic compartments as PDF is expressed in the cytoplasm.[55] In agreement with previous studies,[56] we observed that the majority of TIM was cytoplasmic at ZT16 in *tim*(WT) flies but became progressively more nuclear from early to late night (Figures 2A and 2B). In contrast, *tim*(S1404A) flies displayed significantly lower percentage of nuclear TIM (% nuclear TIM/total TIM) at late night (ZT20 and ZT22; Figure 2B), although phosphomimetic *tim*(S1404D) mutants exhibited higher percentage of nuclear TIM over *tim*(WT) flies at ZT16 and ZT22.

In addition to assessing the distribution of TIM in the nucleus versus cytoplasm, we also monitored overall nuclear TIM abundance. We observed a substantially lower abundance of nuclear TIM in *tim*(S1404A) flies between ZT18 and ZT22, although that in *tim*(S1404D) flies appeared higher than *tim*(WT) at ZT16 to ZT18 but lower at ZT22 (Figures 2A and 2C). Taken together, our results suggest that TIM(S1404) phosphorylation promotes TIM nuclear accumulation and the molecular mechanisms underlying the short-period behavioral phenotypes of *tim*(S1404A) and *tim*(S1404D) flies are likely different.

TIM(S1404) Phosphorylation Regulates TIM-XPO1 Interaction

A number of studies have established that PER-TIM nuclear accumulation is regulated by phosphorylation.[20,24,28–31,56] With the characterization of TIM nuclear import pathway[12] and functional NLS,[23] phosphorylation has been thought to influence nuclear entry. However, the evidence that nuclear PER-TIM can be translocated back to the cytoplasm[11,19] raises the possibility that phosphorylation may also regulate nuclear export to influence overall levels of nuclear accumulation. To determine whether S1404 phosphorylation regulates TIM nuclear entry or export, we first searched for potential NLS and nuclear export signal (NES) in the sequences adjacent to S1404 based on classical NLS/NES motifs.[57,58] Whereas we did not locate any sequences that resemble an NLS near S1404, we identified one putative NES (L1394-V1403) immediately adjacent to the S1404 residue (Figure 3A). Previous studies suggest that phosphorylated residuê) within or in close proximity to an NES can regulate protein nuclear-cytoplasmic distribution by modulating the binding of cargo protein and chromosome maintenance 1 (CRM1).[59,60] CRM1 is the major export protein in mammals that facilitates the transport of proteins from the nucleus to the cytoplasm.

We therefore tested whether TIM(S1404) phosphorylation reduces the interaction between TIM and XPO1, the *Drosophila* homolog of mammalian CRM1, by performing coimmunoprecipitation (coIP) assays using *Drosophila* S2 cells coexpressing *tim*(WT)-

hemagglutinin (HA) or *tim*(S1404A)-HA with *xpo1*-FLAG and *per*-V5. We observed significantly higher TIM(S1404A)-XPO1 interaction as compared to TIM(WT) when we pulled down TIM-HA and detected the presence of interacting XPO1 (Figures 3B and 3C). We also performed the reciprocal coimmunoprecipitation, which yielded the same conclusion (Figures 3B and 3D). Furthermore, we assayed the binding of TIM(S1404D) to XPO1 and observed that it was significantly lower when compared to that of TIM(S1404A) but similar to the levels for TIM(WT) (Figure S3). The similarity between the interactions between TIM(WT)-XPO1 and TIM(S1404D)-XPO1 can be explained by the confirmation that TIM(S1404) is phosphorylated in TIM(WT) expressed in *Drosophila* S2 cells using a pS1404 phosphospecific antibody we generated for this study (Figures S4A and S4B). The stronger interaction of XPO1 to TIM(S1404A) as compared to TIM(WT) or TIM(S1404D) was further confirmed by glutathione S-transferase (GST)-XPO1 pull-down assay using fly head extracts (Figures 3E and 3F). Taken together, our results suggest that TIM(S1404) phosphorylation inhibits the nuclear export of TIM via the XPO1-dependent pathway.

TIM(S1404) Phosphorylation Increases PER Nuclear Accumulation

Because TIM is necessary for promoting the nuclear entry of PER-TIM heterodimers,[12,22,23] we next sought to determine whether PER nuclear accumulation is also altered in *tim*(S1404A) and *tim*(S1404D) mutants. We monitored subcellular localization of PER in adult clock neurons using the same method as described for TIM. As expected, the percent of nuclear PER (% nuclear PER/total PER) gradually increased from ZT16 to ZT22 in *tim*(WT) flies (Figures 4A and 4B). In comparison, the percent of PER in the nucleus in *tim*(S1404A) mutants was significantly lower at ZT22 although that for *tim*(S1404D) mutant was significantly higher at ZT22. Furthermore, the overall abundance of nuclear PER was also significantly lower in *tim*(S1404A) mutants at ZT22 (Figures 4A and 4C). Our results therefore support that alterations in TIM subcellular localization due to phosphorylation defect at TIM(S1404) impact subcellular localization of its heterodimeric partner PER.

We next compared PER and TIM protein profiles in head extracts of WT and mutants to determine whether altered nuclear accumulation affects their daily rhythms in protein abundance and phosphorylation state. Consistent with previous studies, newly synthesized PER and TIM in *tim*(WT) flies were hypophosphorylated between ZT8 and ZT12 and became progressively more phosphorylated from early night to the following morning (Figures 4D and 4F).[24,25,61] Daily rhythms in PER and TIM protein abundance were altered in *tim*(S1404A) mutants, as determined by detection of differential rhythmicity (DODR) analysis (PER: $p < 0.05$; TIM: $p < 0.01$).[62] In congruence with the short-period phenotype of *tim*(S1404A) flies, the peak phases of both PER and TIM rhythms advanced from ZT20 in *tim*(WT) flies to ZT16 (Figures 4D and 4E) as calculated by rhythmicity analysis incorporating nonparametric methods (RAIN).[63] In addition, daily PER protein rhythmicity was dampened in *tim*(S1404A) mutants (WT: $p < 0.0001$; S1404A: $p = 0.1361$, RAIN). This is likely caused by compromised nuclear accumulation of the PER-TIM proteins, which is clearly affecting their phosphorylation programs and is expected to impact their phase-specific functions. Furthermore, phase advance of *per* and *tim* mRNA, discussed in the next section, is also expected to contribute to changes in PER and TIM proteins rhythms.

In the case of the short-period *tim*(S1404D) mutant, daily rhythms in PER and TIM were significantly altered as compared to *tim*(WT) (PER: $p < 0.05$; TIM: $p < 0.05$, DODR). The peak phase of PER advanced from ZT20 to ZT16 although that for TIM remained unchanged, as determined by RAIN (Figures 4F and 4G). Moreover, we observed significant dampening of the daily rhythmicity of PER proteins in *tim*(S1404D) flies (WT: $p < 0.0001$; S1404D: $p = 0.0720$, RAIN). Daily rhythmicity of TIM in *tim*(S1404D) mutants was slightly dampened as compared to *tim*(WT) although still rhythmic (WT: $p < 0.0001$; S1404D: $p < 0.0001$, RAIN). Notably, the accelerated PER and TIM turnover in *tim*(S1404D) flies at night (Figure 4G) is consistent with their increased nuclear localization at ZT22 (Figures 2B and 4B). Together, our data suggest that TIM(S1404) phosphorylation promotes PER nuclear accumulation indirectly by increasing TIM nuclear retention.

TIM(S1404) Phosphorylation Influences Rhythmic CLK Phosphorylation and Occupancy at Clock Gene Promoter

We next examined whether reduced PER-TIM nuclear accumulation in *tim*(S1404A) mutants affects the output of the molecular oscillator by assaying *per* and *tim* mRNAs. The daily rhythms in *per* and *tim* mRNAs in *tim*(WT) and *tim*(S1404A) mutants were significantly different (PER: $p < 0.001$; TIM: $p< 0.001$, DODR; Figure 5A). Given the reduction of nuclear PER to repress CLK-CYC transcriptional activity in *tim*(S1404A) flies at night, we expect *per* and *tim* mRNA levels in *tim*(S1404A) to be higher when compared to *tim*(WT) flies during the circadian repression phase (~ZT16-ZT24).[16] Surprisingly, *per* and *tim* mRNA levels were substantially lower at ZT16 and ZT20 in the *tim*(S1404A) mutant. In addition, we observed a significant phase advance in *per* mRNAs in *tim*(S1404A) flies, in congruence with the short-period phenotype of this mutant (WT: peak = ZT16; S1404A: peak = ZT12, RAIN). This resulted in significantly higher levels of *per* and *tim* mRNAs at ZT8 (Figure 5A).

Our analysis of clock gene expression clearly suggests that the short-period phenotype of *tim*(S1404A) is driven primarily by the phase advance of CLK transcriptional activity. But how does reduced nuclear accumulation of PER-TIM heterodimers lead to premature activation of CLK transcriptional activity? CLK transcriptional activity has previously been shown to correlate with CLK phosphorylation status.[15,64–69] Subsequent to nuclear translocation of PER-TIM heterodimers, kinases recruited by the PER-TIM complex have been proposed to phosphorylate CLK and inactivate its transcriptional activity.[15,69] Dephosphorylation by phosphatase then produces hypophosphorylated, transcriptionally active CLK the following morning.[70] Because TIM(S1404A) mutation reduces PER-TIM nuclear accumulation (Figures 2B and 4B), we decided to examine its impact on the daily oscillation of CLK phosphorylation (Figures 5B and 5C). We observed significant alteration in the daily rhythm of CLK phosphorylation in *tim*(S1404A) as compared to *tim*(WT) flies ($p < 0.001$, DODR), despite no significant change in CLK abundance (Figure S5A). Specifically, *tim*(S1404A) exhibited significant dampening in the daily CLK phosphorylation rhythms as compared to *tim*(WT) flies (WT: $p < 0.0001$; S1404A: $p = 0.1079$, RAIN). In particular, significantly less hyperphosphorylated CLK isoforms were detected at ZT24/0 and ZT4 in *tim*(S1404A) flies, the time when CLK is predominantly hyperphosphorylated in *tim*(WT) flies (Figures 5B and 5C). Because hypophosphorylated or

intermediately phosphorylated CLK proteins have higher transcriptional activity,[15,68] our results could explain the phase advance in CLK activation of *per* and *tim* expression in *tim*(S1404A) flies (Figure 5A).

We then asked whether reduction in early-morning CLK phosphorylation in *tim*(S1404A) mutants influences CLK occupancy at clock gene promoters and contributes to premature initiation of *per* and *tim* expression. We performed CLK chromatin immunoprecipitation (CLK-ChIP) followed by qPCR using extracts from adult fly heads (Figure 5D). We observed significantly higher CLK occupancy at multiple morning time points at *tim* E-box in the *tim*(S1404A) mutant as compared to that in *tim*(WT) flies. Together, our data suggest that TIM(S1404) phosphorylation can impact daily rhythms in CLK phosphorylation status and transcriptional activity to regulate circadian timekeeping.

In the case of *tim*(S1404D) flies, although daily rhythms in *per* and *tim* mRNAs were not significantly different from *tim*(WT) flies (per: $p = 0.1742$; *tim*: 0.4254, DODR), the peak phase of *per* mRNA was advanced from ZT16 to ZT12 (RAIN), and the repression of both *per* and *tim* appeared to occur earlier (Figure S6A). This may contribute to the advanced peak phase in PER protein rhythms in *tim*(S1404D) flies (Figures 4F and 4G). Because CLK protein abundance was not significantly altered in *tim*(S1404D) mutants (Figure S5B), the advanced peak phase of *per* mRNA is likely a consequence of alteration in CLK phosphorylation rhythm. In agreement with our hypothesis, the amount of hyperphosphorylated CLK in *tim*(S1404D) was significantly lower at ZT4, which is expected to result in higher CLK transcriptional activity. Finally, we observed an apparent decrease in the amplitude of daily CLK phosphorylation rhythm in *tim*(S1404D) as compared to WT, but it was not significantly altered ($p = 0.3140$, DODR; Figures S6B and S6C).

CK2 Kinase Phosphorylates TIM(S1404)

We next sought to identify the kinase that phosphorylates TIM(S1404). Based on KinasePhos 2.0,[71] CK2 is predicted with the highest probability to phosphorylate S1404 (Figure 6A). To confirm this *in silica* prediction, we generated a S1404 phosphospecific antibody (α-pS1404) using a phosphorylated S1404-containing peptide as antigen. We then assayed TIM(S1404) phosphorylation in protein extracts of *Drosophila* S2 cells coexpressing *tim*-HA (WT or S1404A) with either the catalytic subunit of *ck2* (*ck2α*) or a dominant-negative variant *ck2α*(*tik*).[26,30] Immunoblotting showed that TIM(pS1404) was significantly reduced when *tim*(WT)-HA was coexpressed with *ck2α*(*tik*) as compared to coexpression with *ck2α*(WT) (Figures 6B, lanes 2 to 3, and 6C). Moreover, there was little to no α-pS1404 signal detected in *tim*(S1404A) (Figures 6B, lanes 4–6, and 6C), suggesting the α-pS1404 antibody is phosphospecific. To further validate the specificity of α-pS1404, we confirmed the reduction of α-pS1404 isoforms when TIM was immunoprecipitated and phosphatase treated prior to immunoblotting (Figures S4A and S4B, lanes 1 to 2).

We proceeded to test whether downregulating CK2 activity in flies reduces TIM(S1404) phosphorylation. First, we evaluated TIM(S1404) phosphorylation over a daily cycle and observed that phosphorylation at TIM(S1404) was detected at ZT16 and ZT20 in *tim*(WT) but absent in *tim*(S1404A) flies (Figure 6D). Next, we genetically knocked down CK2

activity by overexpressing *ck2α*(*tik*) in clock neurons using the *tim*-UAS-Gal4 driver (*TUG*).[72] Head extracts from *TUG* > UAS-*ck2α*(*tik*) flies and parental controls collected at ZT20 were probed for S1404 phosphorylation. In concordance with the results in S2 cells, we observed a significant reduction in S1404 phosphorylation in *ck2α*(*tik*)-overexpressing flies (Figures 6E and 6F). Taken together, our results suggest that CK2 phosphorylates TIM(S1404) in *tim*-expressing clock neurons.

Finally, we performed immunocytochemistry in adult brain clock neurons to investigate the subcellular localization of CK2-dependent phosphorylation of TIM(pS1404). Based on western blotting results (Figure 6D) and MS data (Table S1) showing TIM(S1404) phosphorylation at ZT16 in whole-head extracts, abundant cytoplasmic localization of CK2,[26] and previous studies indicating the role of CK2 in promoting PER-TIM nuclear import,[26,27,30,31] we hypothesize that CK2 first phosphorylates TIM at S1404 and residues important for nuclear import in the cytoplasm. This and the role of TIM(S1404) phosphorylation in inhibiting nuclear export are not mutually exclusive. In agreement with our observation from whole-head extracts, we observed prominent TIM(pS1404) signal in clock neurons at ZT16 in *tim*(WT), but not in *tim*(S1404A) mutants (Figure S4C).

DISCUSSION

To better understand the role of phosphorylation in regulating the function of the PER-TIM heterodimer, we identified multiple phosphorylation sites on PER-bound TIM proteins extracted from *Drosophila* tissues. After an initial behavioral screen of *tim* non-phosphorylatable mutants, we proceeded to characterize the function of TIM(S1404), which is located in the TIM CLD and is predicted to be phosphorylated by CK2, a known clock kinase. Leveraging the results from a series of molecular and behavioral analyses on transgenic flies expressing *tim*(S1404A) and *tim*(S1404D) mutants, we formulated a model describing the function of CK2-dependent TIM(S1404) phosphorylation in the molecular clock (Figure 7). In WT flies, TIM(S1404) is first phosphorylated by CK2 in the cytoplasm in early night. Our data do not rule out the possibility that CK2-dependent phosphorylation of TIM(S1404) continues after the entry of PER-TIM heterodimer into the nucleus around midnight. After nuclear entry, TIM(S1404) phosphorylation inhibits the interaction of TIM and the nuclear export machinery, thereby promoting nuclear accumulation of PER-TIM heterodimers. This facilitates timely CLK phosphorylation by kinases recruited by the PER-TIM complex to enhance circadian repression. The identity of kinase(s) that serve this role will need to be resolved in future investigations. Hyperphosphorylated CLK is then dephosphorylated by the CKA-PP2A complex[70] in the following morning to activate the next round of clock gene expression.

Our model is consistent with previous studies showing that PER-TIM-DBT complexes recruit as yet unknown kinases to phosphorylate CLK.[69] It is also consistent with studies proposing that CK2 regulates PER function by phosphorylating TIM.[30,31] Because the S1404A mutation results in a short-period phenotype, which is opposite to the period-lengthening effect of $ck2\alpha^{tik}$,[26] our results highlight the complex functions of CK2 in regulating the molecular clock.

In *tim*(S1404A) mutants, the nuclear entry of PER-TIM heterodimer is not affected and proceeds as normal around midnight. Once in the nucleus, TIM(S1404A) interacts with the nuclear export machinery with higher affinity as compared to TIM(WT), leading to increased nuclear export and higher percentage of PER-TIM heterodimers in the cytoplasm. As a result, CLK phosphorylation in the nucleus is reduced, as there are less PER-TIM heterodimers available to serve as scaffolds to recruit CLK kinases. In agreement with this model, we observed dampening of daily CLK phosphorylation rhythms in *tim*(S1404A) flies (Figure 5B). Specifically, there is significantly lower level of hyperphosphorylated CLK isoforms in late night to early morning. Given that CLK hyperphosphorylation is linked to reduced transcriptional activity, it is somewhat surprising that reduced CLK phosphorylation at night (ZT20–ZT24) did not significantly enhance clock gene expression (Figure 5A). This supports that other modifications, such as ubiquitination, are also important for regulating CLK transcriptional activity.[73] USP8 has been shown to deubiquitylate CLK at late night to facilitate repression of clock genes.

We propose that reduced CLK hyperphosphorylation represents the key driver for the short-period phenotype of *tim*(S1404A) mutant. Because CLK is not hyperphosphorylated by kinases recruited by the PER-TIM heterodimers at night, it does not have to be dephosphorylated by the CKA-PP2A complex[70] in the morning of the next cycle to activate clock gene transcription. This would explain the phase advance of CLK occupancy on circadian promoters (Figure 5D) and CLK-activated *per* and *tim* expression (Figure 5A). It is interesting to note that we did not observe diminished repression of clock genes despite the reduction of nuclear PER-TIM heterodimers at night (Figure 5A), indicating additional mechanisms, e.g., chromatin remodeling and protein modifications, that are absent during this time of the circadian cycle are necessary to activate clock gene expression, even when the level of PER repressor is reduced.

Curiously, *tim*(S1404D) mutants also exhibit a short-period phenotype in behavioral rhythms (Figure 1B). The fact that *tim*(S1404D) mutants display the opposite molecular phenotype in the context of nucleocytoplasmic localization of TIM and PER when compared to *tim*(S1404A) flies support that the S1404D mutation is phosphomimetic (Figures 2 and 4). The short-period phenotype of the *tim*(S1404D) mutant is therefore best explained by phase advance of the nuclear accumulation and subsequent degradation of PER-TIM heterodimer due to sustained inhibition of TIM-XPO1 interaction. Because of accelerated PER-TIM degradation, the time frame for PER-TIM to recruit CLK kinases is shortened. This would explain the significantly lower amount of hyperphosphorylated CLK in *tim*(S1404D) flies at ZT4 and the phase advance of *per* mRNA rhythm (Figure S6).

Previous studies suggested that TIM phosphorylation plays a role in regulating its light-dependent degradation as well as its subcellular localization. Phosphorylation of tyrosine (pY) was first proposed to precede the degradation of TIM upon light exposure.[40] We did not recover any pY residues in our MS analysis of PER-bound TIM. Nevertheless, we cannot rule out that Y phosphorylation may occur when TIM is not in complex with PER. Furthermore, it is possible that pY may result in the disassembly of the PER-TIM heterodimer or could result in very unstable TIM proteins that are difficult to purify from fly tissues. Instead of potential pY residues, we were able to identify a number of

phosphorylated S/T residues that significantly impact behavioral phase shift responses to a light pulse at ZT15 or ZT21, suggesting they may be involved in mediating light-dependent TIM degradation (Figures S1C and S1D). TIM(S568) is located within a functional NLS.[23] Non-phosphorylatable *tim*(S568A) mutants exhibited arrhythmic locomotor activity (Figure 1B), which is consistent with the phenotype of mutants defective in TIM nuclear entry[22,23] and/or light entrainment.[22] Future investigations are necessary to determine whether S568 phosphorylation may regulate TIM subcellular localization and/or light responses. It will be also interesting to determine whether phosphorylation at S1389, S1393, and S1396, which are close to the NESs identified in this study, play a role in regulating TIM nuclear export. Of note, we did not observe phosphorylation at T113, S297/T301, and T305/S309/S313 residues in our MS analysis. These residues were previously suggested to promote TIM nuclear entry when phosphorylated.[22,31] It is possible that these residues are more highly phosphorylated when TIM is not bound to PER.

In summary, we describe a phosphorylation-dependent nuclear export mechanism that regulates the nuclear accumulation of PER-TIM heterodimers and consequently the phase of CLK transcriptional activity in the molecular clock. We identified an NES motif in the previously characterized TIM CLD domain and showed that S1404 phosphorylation adjacent to this NES can regulate PER-TIM nuclear export. NES has been shown repeatedly to be an important regulatory motif that modulates localization and activities of transcriptional repressor in eukaryotes.[74–78] The NES and S1404 module at the C terminus of TIM is highly conserved in drosophilids and in most species that have the *timeless* gene (Figures S2A and S2B). Together with our MS analysis showing the phosphorylation of *Danaus plexippus* TIM(S1174), the homologous site of *Drosophila melanogaster* TIM(S1404) (Figure S2C), we expect this phosphorylation-dependent mechanism that regulates TIM function to be conserved in insects. Interestingly, in *timeout/timeless 2* (homolog of mammalian *timeless*), the ancestral paralog of *tim* that has a role in circadian photoreception, but not in the oscillator itself,[79,80] this C-terminal NES is absent and serine is replaced by a glutamic acid (E) (Figure S2B). We speculate that the gain of the NES and TIM(S1404) module at some point in evolution likely enabled TIM to cycle between subcellular compartments in a phosphorylation- and phase-dependent manner over the circadian cycle. This would allow CK2-dependent TIM phosphorylation to regulate the phase-specific functions of PER-TIM heterodimers in specific lineages.

Finally, it is interesting to point out that a mutation in mammalian *timeless* that results in decreased nuclear TIM accumulation also leads to phase advance of human sleep-wake behavior, an output of the circadian clock.[81] The circadian period length of mice expressing the TIM(R1081X) mutation, which manifests into human familial advanced sleep phase syndrome (FASPS), as determined by activity rhythm, is identical to WT mice. However, proliferating embryonic fibroblasts derived from heterozygous TIM(R1081X) mutant mice as well as mammalian U2OS and HEK293 cells expressing this same mutation exhibit a significant period shortening. This suggests that decreased TIM nuclear accumulation in flies and mammals results in similar outcomes in the context of the molecular clock. Our results highlight an unexpected parallel between the functions of *Drosophila* and mammalian *timeless* in the molecular clock, even though the exact mechanisms and sequence motifs regulating their functions might have diverged. Analysis of *Drosophila tim* mutants could

provide insights into the mechanisms that regulate the nuclear accumulation of mammalian TIM and further elucidate its functions in the mammalian clock. For instance, similar to what we deduced from *Drosophila tim*(S1404A) mutant, the advanced sleep phenotype in human FASPS R1081X patients could be the result of altered phosphorylation profile of BMAL1-CLOCK, leading to phase advance in circadian transcriptional activation.

STAR★METHODS

RESOURCE AVAILABILITY

Lead Contact—Further information and requests for resources and reagents should be directed to and will be fulfilled by the lead contact Joanna C. Chiu (jcchiu@ucdavis.edu).

Materials Availability—All unique/stable reagents generated in this study are available from the lead contact without restriction.

Data and Code Availability—This manuscript includes all datasets generated or analyzed during this study. Proteomics data have been deposited into public data repository. Accession numbers are provided in Method Details.

EXPERIMENTAL MODEL AND SUBJECT DETAILS

***Drosophila* construct design and transformation—**A *p*{*tim*{WT)-*luc*} transgene, containing 4.1kb of the *tim* promoter, *tim* full-length cDNA (*Is-tim* allele), and a luciferase reporter in the *pattB* vector, was kindly provided by Patrick Emery. The luciferase reporter was removed using MluI/XhoI restriction sites, and a 3XFLAG-6XHIS epitope was added in frame to the C terminus of the *tim* coding region. PhiC31 site-directed recombination[88] was used for transgenesis to generate *yw*; *tim*^{0}; *tim*(WT) (also described in[82]). Plasmids were injected into *yw* fly embryos carrying *attP* sites on chromosome 3 (*attP2*) (BestGene, Chino Hills, CA). Transformants were crossed with *yw*; *tim*^{0} flies[53] to remove endogenous copies of *tim* prior to behavioral and molecular analyses. To generate flies expressing non-phosphorylatable (Serine/Threonine (S/T) to Alanine (A)) or phosphomimetic (S/T to Aspartic acid (D)) *tim* mutants, pAc-*Is-tim*-HA was used as the template for site-directed mutagenesis using Pfu Turbo Cx DNA polymerase (Agilent Technologies, Santa Clara, CA) (see Table S3 for mutagenic primer sequences). After mutagenesis and confirmation by Sanger sequencing (UC Davis DNA Sequencing Facility), the mutant variants of 2.8 kb MluI-XbaI *tim* subfragments were used to replace the corresponding WT fragments in *pattB-p*{*tim*(WT)-3XFLAG-6XHIS}.

Targeted expression of *ck2α* dsRNA in *tim*-expressing neurons was achieved via the UAS/Gal4 system[89]. The Gal4 driver line, *w; UAS-dicer2; tim-UAS-Gal4* (*TUG*)[72], was used to drive expression in *tim* expressing clock neurons. *UAS-ck2α*^{tik} responder line (B24624) from the Bloomington *Drosophila* Stock Center was used to reduce endogenous function of CK2α.

METHOD DETAILS

Identification of TIM PTM sites from fly tissues—PER-bound TIM phosphorylation and O-GlcNAcylation sites were identified from the label-free mass spectrometry (MS) proteomics experiments as previously described[47]. Procedures for immunoprecipitation of PER-TIM complexes and mass spectrometry (MS) were previously described[47]. Epitope-tagged PER proteins were pulled down using α-FLAG and PER-bound TIM proteins were pulled down simultaneously and subjected to MS analysis.

Mass spectrometric data was analyzed with PEAKS Studio X+ (Bioinformatics Solutions Inc., Canada). Raw data refinement was performed with the following settings: Merge Options: no merge, Precursor Options: corrected, Charge Options: 1-6, Filter Options: no filter, Process: true, Default: true, Associate Chimera: yes. *De novo* sequencing and database searching were performed with a Parent Mass Error Tolerance of 10 ppm. Fragment Mass Error Tolerance was set to 0.02 Da, and Enzyme was set to none. The following variable modifications were applied: Oxidation (M), pyro-Glu from Q (N-term Q), phosphorylation (STY), acetylation (protein N-terminal) and HexNAc (STNY). Carbamidomethylation (C) was set as fixed modification. A maximum of 5 variable PTMs were allowed per peptide. A custom database of appropriate size (550 protein sequences) containing TIMELESS protein sequence (UniProt ID A0A1W5PW00) from UniProt was used for database searching. Database search results were filtered to 1% PSM-FDR. Phosphosite localization was validated by inspecting fragment ion spectra of all phosphopeptides. Identification of GlcNAc-modified peptides was confirmed by inspecting the corresponding fragment ion spectra for the presence of characteristic fragment ions (m/z 168.07, 186.08, 204.09). The *Drosophila* MS data has been deposited into Chorus repository (project ID 1424): (https://chorusproject.org/anonymous/download/experiment/e47a30f7f2c749aba438652d7d88ef04) and (https://chorusproject.org/anonymous/download/experiment/e6d6163b31bf40288606f827c6f18371)

***Danaus plexippus* DpN1 cell culture—**Monarch butterfly DpN1 cells[85], kindly provided by Steven Reppert and Christine Merlin, were grown at 28°C in Grace's medium (Thermo Fisher Scientific, Waltham, MA), supplemented with 10% Fetal Bovine Serum (FBS) (VWR, Radnor, PA) and 1X penicillin/streptomycin (Thermo Fisher Scientific). Cells were passed every 7 days. Old medium was removed and cells were washed with cell culture grade 1XPBS (Thermo Fisher Scientific) once before treating with Trypsin/EDTA (Thermo Fisher Scientific) for at least two minutes at 28°C. To halt trypsinization, FBS-containing Grace's medium was added to the cells. Cell suspensions were then passed into new tissue culture flask with FBS-containing Grace's medium.

AP-MS of *Danaus plexippus* PER and TIM—For each time-point, roughly 2.5g of cell pellet in Lysis Buffer (20mM HEPES pH 7.5, 1mM DTT, 0.5mM PMSF and SIGMAFAST EDTA-free protease inhibitor cocktail (Sigma) weredounced prior to centrifugation at 800xg for 15 minutes at 4°C to separate nuclear and cytoplasmic fractions. The nuclear fraction (pellet) was washed twice with Lysis Buffer prior to resuspension in Nuclear Extraction Buffer (20mM Tris-HCl pH 7.5, 150mM NaCl, 0.5mM EDTA, 1mM DTT, 1mM $MgCl_2$, 1% Triton X-100, 0.4% sodium deoxycholate, 0.5mM PMSF, 10mM NaF, 10% glycerol and

SIGMAFAST EDTA-free protease inhibitor cocktail) and dounced with tight pestle supplemented with MG132 (Sigma) and DNase I (Promega, Madison, WI). The cytoplasmic fraction (supernatant) was supplemented with 150mM NaCl, 1mM $MgCl_2$, 0.5mM EDTA, 1% Triton X-100, 0.4% sodium deoxycholate, 10mM NaF, 10% glycerol and SIGMAFAST EDTA-free protease inhibitor cocktail. After 30 minutes incubation at 4°C, nuclear fraction was diluted to 0.1% SDS with concentration of other content unchanged. Nuclear and cytoplasmic fractions were then centrifuged at 15,000 rpm for 15 minutes. Supernatants were incubated with gammabind Sepharose beads (GE Healthcare, Piscataway, NJ) for 30 minutes at 4°C to reduce nonspecific binding prior to overnight incubation with α-DpPER (GP5913, RRID: AB_2832970). On the second day, samples were incubated with gammabind Sepharose beads (GE Healthcare). Beads were washed three times with Wash buffer (20mM HEPES, 150mM NaCl, 1mM $MgCl_2$, 1mM DTT, 0.5mM EDTA, 1% Triton X-100, 0.4% sodium deoxycholate, 10mM NaF, 0.5mM PMSF, 10% glycerol) and subsequently eluted in 200ul 2X SDS sample buffer at 95°C for 4 minutes. After resolving eluates on a Tris-Tricine gel, excised gel containing eluates was digested with protease and followed by mass spectrometry as previously described[47]. DpTIM was copurified with DpPER and analyzed by MS. DpN1 MS data has been deposited into ProteomeXchange (ftp://massive.ucsd.edu/MSV000085748/).

Locomotor activity assay—Daily locomotor activity rhythms in male flies was assayed using the *Drosophila* Activity Monitoring System (DAMS, Trikinetics, Waltham, MA) as described previously[90]. Young adult male flies (~3-5-day old) were entrained for 4 days in light/dark (LD) cycles (12h light/12h dark), followed by 7 days of constant darkness (DD) to assess their free-running rhythms in incubators at 25 C. Each fly was kept in 5mm glass tube that contains fly food, 5% Sucrose, 2% Bacto Agar (BD Biosciences, San Jose, CA), atone end and plugged with yarn at the other end. The locomotor activity data from individual flies were analyzed using the FaasX software (Fly Activity Analysis Suite for Mac OSX). Periods of each fly were calculated using the chi-square periodogram analysis and pooled for a composite for each genotype.

Assaying responses to light pulse—Male flies were entrained for 4 days in LD cycle (12h light/12h dark). In the dark phase on LD4, the light-pulsed (LP) flies were given a 10-minute pulse of light at ZT15 or ZT 21 before being placed in 7 days of DD, while the non-light pulsed (NLP) flies were not exposed to light pulse treatments. Activity rhythms were measured using the DAMS and analyzed as using FaasX as described in the locomotor activity assay section. Peaks in activity rhythms were restricted to between ZT 6 and ZT 18 and converted into a value in degrees using Excel (Microsoft, Redmond, WA) (24 hours = 360°). LD3 data was used to normalize the DD1 data of each fly by subtracting the LD3 from DD1, within each respective genotype. *tim*(WT) degree values were then subtracted from each mutant to determine the phase shift as a result of the light pulse. The difference in degrees was then converted back to hours using Excel (Microsoft).

Plasmids for *Drosophila* S2 cell culture—*Exportin 1* (*xpo1*) ORF was amplified from cDNA that was reverse transcribed (Superscript IV, Thermo Fisher Scientific) from total

RNA extracted from fly heads using TRI Reagent (Sigma, St. Louis, MO). The PCR product was cloned into pAc-3XFLAG-6XHIS[42] and pMT-*gst*[41].

Drosophila S2 cell culture and transfection—*Drosophila* S2 cells and *Schneider's Drosophila* medium were obtained from Life Technologies (Carlsbad, CA). For all cell culture experiments, S2 cells were seeded at 1 X 10^6 cells/ml in a 6-well plate and transfected using Effectene (QIAGEN, Germantown, MD). For coimmunoprecipitation (coIP) assays, S2 cells were co-transfected with 0.8 μg of pAc-*per*-V5-HIS (herein referred to as pAc-*per*-V5), 0.8 μg of pAc-*xpo1*-3XFLAG-6XHIS (herein referred to as pAc-*xpo1*-FH) and 0.8 μg of pAc-*tim*(X)-HA, where X is either WT or S1404A to detect protein-protein interactions. In control IPs to detect non-specific binding, cells were co-transfected with pAc-*per*-V5-His and pAc-*xpo1*-FH without pAc-*tim*(X)-HA. S2 cells were harvested 40 hours after transfection. For GST pull-down assays, S2 cells were transfected with either 0.8 μg of pMT-*gst-xpo1* or 0.8 μg of pMT-*gst* and induced with 500 μM $CuSO_4$ immediately after transfection and cells were harvested 44 hours after induction. For IP to detect TIM(pS1404), S2 cells were co-transfected with 0.8 μg of pAc-*tim*(X)-HA and either 0.2 μg of pMT-*ck2α*-V5 or 0.2 μg pMT-V5-His as empty control. Expression of *ck2α* was induced with 500 μM $CuSO_4$ immediately after transfection and cells were harvested 40 hours after kinase induction.

Coimmunoprecipitation in _Drosophila_ S2 cells—CoIP experiments were performed as described previously[10] with the following modifications. Cells were harvested 40 hours after transfection, washed once with 1X PBS and lysed with modified RIPA(20mM Tris-HCl pH 7.5, 150mM NaCl, 10% glycerol, 1% Triton X-100, 0.4% sodium deoxycholate, 0.1% SDS, 1mM EDTA) supplemented with 25mM NaF, 0.5mM PMSF, and SIGMAFAST EDTA-free protease inhibitor cocktail. Proteins were incubated with 20 μL α-HA or α-FLAG M2 resins (Sigma) for 4 hours at 4°C to pull down TIM or XPO1, respectively. Resins were washed three times in modified RIPA buffer. Immune complexes were analyzed by western blotting. Signal intensity of interacting protein was normalized to the intensity of the bait protein.

GST pull-down assays using fly head extracts—GST pull-down assays were performed as previously described[41] with the following modifications. GST Lysis Buffer (20mM Tris-HCl pH 7.5, 0.05% IGEPAL CA-630 (Sigma), 1mM EDTA, 5mM DTT, 150mM NaCl, 25mM NaF) was used for protein extractions from S2 cells. Extracts containing GST or GST-XPO1 were incubated with 25 μL glutathione Sepharose beads (GE healthcare) for 6 hours at 4°C. Beads were washed two times in GST Lysis Buffer and once with modified RIPA buffer. Prey proteins were extracted from 500 μL of fly heads per reaction with modified RIPA buffer and incubated with GST- or GST-XPO1-bound beads for 6 hours. Beads were washed three times in modified RIPA buffer. Input and bound TIM were analyzed by western blotting.

Western blotting and antibodies—Protein extractions from *Drosophila* S2 cells and adult fly heads, western blotting, and image analysis was performed as previously described[41,83]. RBS buffer (20mM HEPES pH7.5, 50mM KCl, 10% glycerol, 2mM EDTA,

1mM DTT, 1% Triton X-100, 0.4% NP-40, 10 μg/ml Aprotinin, 5 μg/ml Leupeptin, 1 μg/ml Pepstatin, 0.5mM PMSF, 25mM NaF) was used for protein extractions from fly heads. Protein concentration was measured using Pierce Coomassie Plus Assay Reagents (Thermo Fisher Scientific). 2X SDS sample buffer was added and the mixture boiled at 95°C for 5 minutes. Equal amounts of proteins were resolved by polyacrylamide-SDS gel electrophoresis (PAGE) and transferred to nitrocellulose membrane (Bio-Rad, Hercules, CA) using Semi-Dry Transfer Cell (Bio-Rad). Membranes were incubated in 5% Blocking Buffer (Bio-Rad) for 40 minutes, incubated with primary antibodies for 16-20 hours. Blots were then washed with 1X TBST for 1 hour, incubated with secondary antibodies for 1 hour, washed again prior to treatment of chemiluminescence ECL reagent (Bio-Rad). The following percentage of polyacrylamide-SDS gel were used: 6% for PER, TIM; 8% for CLK and XPO1, 10% for HSP70 and 12% for CK2α.

Primary antibodies: α-HA3F10 (Roche, Indianapolis, IN) at 1:2000 for TIM-HA, α-V5 (Thermo Fisher Scientific) at 1:3000 for PER-V5, α-FLAG (Sigma) at 1:7000 for XPO1-FLAG, α-GST (GE Healthcare) at 1:5000 for GST and GST-XPO1, α-TIM (R5839, RRID:AB_2782953) at 1:1000 for TIM^{82}, α-pS1404 (RB S4602-2, RRID:AB_2814716) at 1:2000 for TIM(pS1404) isoforms, α-CLK (GP6139, RRID:AB_2827523) at 1:2000 for CLK, α-PER (GP5620; RRID:AB_2747405) at 1:2000 for PER and α-HSP70 (Sigma) at 1:10000 was used for to indicate equal loading and for normalization. Secondary antibodies conjugated with HRP were added as follows: α-mouse IgG (Sigma) at 1:2000 for α-V5 detection, 1:2000 for α-FLAG detection, or 1:10,000 for α-HSP70 detection, α-goat IgG (Santa Cruz Biotechnology) at 1:3000 for α-GST detection, α-guinea pig IgG (Sigma) at 1:1000 for α-PER detection, α-rabbit IgG (Sigma) at 1:2000 for α-pS1404 detection, and α-rat IgG (Sigma) at 1:1000 for detecting α-HA and α-TIM.

Generating *Drosophila* CLOCK antibodies—The first 1770 nucleotides of *Drosophila clk* cDNA (Flybase: FBpp0099478) was subcloned into a modified His-tagged pFastBac1 vector (Invitrogen, Carlsbad, CA) as previously described[86]. The recombined construct, pFastBac1-6XHis-*dclk* (1-1770), was transformed into DH10BAC *E. coli* (Invitrogen) and bacmid DNA was then purified. To generate viral stock, bacmid DNA was transfected into Sf9 cells using XtremeGENE 9 transfection reagent (Sigma) and media is collected according to the manufacturer's protocol. Viral stock was used to infect Sf9 cells (Thermo Fisher Scientific) for large-scale expression of CLK antigen. As the CLK antigen is insoluble in extraction buffer (20mM HEPES pH 7.5, 400mM KCl, 5mM imidazole, 10% glycerol, 10mM β-mercaptoethanol) supplemented with 1X SIGMAFAST EDTA-free protease inhibitor cocktail, we collected the insoluble cell pellet after extraction and dissolved it in denaturing solution (50mM Na_3PO_4, 1% SDS) by boiling for 10 minutes. SDS in the sample was diluted to 0.05% before purification using 5ml of Ni-NTA Superflow nickle-charged resin (QIAGEN). CLK antigen was sent to Covance Inc. (Princeton, NJ) for antibody production in guinea pigs. Antibody specificity was confirmed by comparing signals in WT and Clk^{out} flies (Figure S5C).

Generating *Danaus plexippus* PERIOD antibodies—*Danaus plexippus per* (*dpper*) cDNA sequence that encodes amino acid 898-1095 was amplified from pBA-*dpper*-FLAG[85]

and subcloned into the pHis::Parallel1 bacterial expression vector kindly provided by Carrie Partch. The BL21 (DE3) *E. coli* strain containing plasmids with *dpper* fragment were grown to an OD_{600} of ~0.7-0.8 in the presence of ampicillin (125 μg/ml) and protein expression was induced as described previously[87]. Protein expression was induced with 0.5mM isopropyl β-D-1-thiogalactopyranoside (IPTG) and incubated for 16-20 hours at 18°C in Luria Broth (Sigma). Cells were lysed in with microfluidizer (Microfluidics, West Wood, MA). Affinity purification was performed using NGC system (Bio-Rad): the soluble fraction of lysate was passed over a 5ml IMAC Nickle column, washed thoroughly, and eluted with 250mM imidazole. Fractions of interest were buffer exchanged into lysis buffer using 3 kDa molecular weight cutoff filters (EMD Millipore, Burlington, MA). Purified dpPER fragment was used as immunogen in guinea pigs (Covance). This antibody has been deposited into the Antibody registry (RRID: AB_2832970).

Generating TIM(S1404) phosphospecific antibodies—Phosphospecific antibodies were generated by ProteinTech Group, Inc (Rosemont, IL). Rabbits were immunized with a 15-amino-acid peptide (amino acid 1397-DLTRMYVpSDEDDRLE-amino acid 1411; where pS = phosphoserine). The resulting rabbit sera was further affinity-purified using the pS1404 phosphopeptide.

Detecting pS1404 in S2 cells and fly extracts—IP and λ-PP treatment were performed as described previously[41]. TIM proteins from S2 cells were extracted using EB2 (20mM HEPES pH 7.5, 100mM KCl, 5% Glycerol, 5mM EDTA, 0.1% Triton X-100, 0.5mM PMSF, 1mM DTT, 10 μg/ml Aprotinin, 5 μg/ml Leupeptin, 1 μg/ml Pepstatin) supplemented with 1X PhosSTOP (Roche) and 25mM NaF, and were pulled down using 20 μL of α-HA resin per IP reaction. IP with fly protein lysates (extracted with RBS supplemented with 1X PhosSTOP) were performed using 4 μL α-TIM and 20ul gammabind Sepharose beads (GE Healthcare) per reaction.

For λ-PP treatment, resin was washed three times with EB2 (without NaF and PhosSTOP), and once with λ-PP buffer (50mM Tris-HCl pH 7.5, 0.1mM EDTA, 5mM DTT, 0,01% Triton X-100, 2mM $MnCl_2$, and 0.1mg/ml BSA). Resin was then split into two and resuspended in 40 μL λ-PP buffer, with half treated with 1 μL λ-PP (NEB) for 30 minutes at 30°C and the other half mock-treated at the same temperature. Immune complexes were then analyzed by western blotting as described above.

Immunofluorescence and confocal imaging—Brain dissections and immunofluorescence staining procedures were performed as described previously[91]. 3-5 day-old flies were entrained for 4 days and fixed with 4% paraformaldehyde for 40 minutes at 2-hour intervals between ZT16 and ZT22. Brains were washed three times in 1XPBST (0.1% Triton X-100 in PBS), blocked with 10% Normal Goat Serum (Jackson Immunoresearch, West Grove, PA) in PBST for 90 minutes and incubated with primary antibodies overnight. Primary antibodies against PDF, PER, and TIM were used at the following dilutions: 1:1500 rabbit α-PER (Gift from Dr. Patrick Emery)[35], 1:100 GP α-TIM (Gift from Dr. Patrick Emery)[84] and 1:400 mouse α-PDF (C7-C; Developmental Studies Hybridoma Bank, Iowa City, IA). Brains were then washed and probed with secondary antibodies at a 1:200 dilution for α-rat-cy3 (Jackson Immunoresearch, 706-165-148), α-

rabbit IgG Alexa Fluor 488 (Jackson Immunoresearch, 711-545-152) and α-mouse-cy5 (Jackson Immunoresearch, 715-175-150). PDF staining was used to label the sLNvs and as a cytoplasmic marker. Total neuron and nuclear TIM staining was quantified based on a single layer of confocal image with the highest TIM signal. Nuclear TIM was determined by the non-overlapping portion of TIM between TIM and PDF signal in each neuron. Eight to ten fly brains for each genotype were dissected and imaged. Representative images are shown. Fiji software was used for image analysis[92].

Quantitative RT-PCR—RNA was extracted from approximately 50 μL of fly heads using 3X volume TRI Reagent (Sigma). 1/5 volume of 100% chloroform (Sigma) was added and incubated at room temperature for 10 minutes. Upper aqueous layer was recovered after spinning down. Same volume of 100% isopropanol was added and incubated at −20C overnight to precipitate RNA. After spinning down, RNA pellet was washed with 70% ethanol once, resuspended in 20 μL 1X RQ1 buffer (Promega), treated with 2 μL RQ1 DNase (Promega) at 37C for 30 minutes prior to the incubation with 2 μL RQ1 DNase stop solution (Promega) at 65C for 10 minutes. cDNA was generated from equal amount of RNA using Superscript IV (Thermo Fisher Scientific). Real-time PCR was performed using SsoAdvanced SYBR green supermix (Bio-Rad) in a CFX96 (Bio-Rad). Three technical replicates were performed for each biological qPCR replicate. Three biological replicates were performed for each experiment.

Chromatin Immunoprecipitation (ChIP)—CLK-ChIP was performed as described previously[83]. All buffers described below, except ChIP Elution buffer, contain 1X SIGMAFAST EDTA-free protease inhibitor cocktail and 0.5 mM PMSF. Briefly, fly head tissues were homogenized using liquid nitrogen chilled mortar and pestle, mixed with Nuclear Extraction buffer (10mM Tris-HCl pH 8.0, 0.1mM EGTA pH 8.0, 10mM NaCl, 0.5mM EDTA pH 8.0,1mM DTT, 0.5% Tergitol NP-10, 0.5mM Spermidine, 0.15mM Spermine), and lysed with a dounce homogenizer. Homogenate was transferred to a 70 μm cell strainer prior to centrifugation at 300 g for 1 minute at 4°C. Supernatant were centrifuged at 6700 rpm for 10 minutes at 4°C. Pellets were resuspended in NEB buffer prior to centrifugation at 11,500 rpm for 20 minutes at 4°C on a sucrose gradient (1.6M sucrose in NEB and 0.8M sucrose in NEB). Nuclei-containing pellets were fixed with 0.3% formaldehyde in NEB and rotated at room temperature for 10 minutes. Glycine was then added at a final concentration of 0.13mM to quench crosslinking. Samples were centrifuged at 6,500 rpm for 5 minutes at at 4°C. Pellets (cross-linked chromatin) were washed twice with NEB and resuspended in Sonication buffer (10mM Tris-HCl pH 7.5, 2mM EDTA pH 8.0,1% SDS, 0.2% Triton X-100, 0.5mM Spermidine, 0.15mM Spermine). The cross-linked chromatin was sheared by sonicator (Q80023, QSonica, Newton, Connecticut) to roughly 500 base pair fragments. Supernatant (sheared chromatin) was collected after the centrifugation at 10,000 rpm for 10 minutes. 1.5 μL of CLK antibodies (generated in this study) were incubated with 25 μL of Dynabeads in ChIP Wash buffer (50mM Tris-HCl pH 7.5, 1mM EDTA pH 8.0, 1% Triton X-100, 0.1% DOC, 10 μg/ml AcBSA (Promega), 100mM KCl in 1X PBS, 150mM NaCl, 5mM EGTA pH 8.0, 0.1% SDS) at 4°C for 2 hours. Following incubation, beads were collected and incubated with sheared chromatin that were diluted 10-fold with IP buffer (50mM Tris-HCl pH 7.5, 2mM EDTA pH 8.0, 1% Triton

X-100, 0.1% DOC, 150mM NaCl, 0.5mM EGTA pH 8.0) at 4°C for 2 hours. Beads were then collected and washed twice with CW buffer for 30 minutes at 4°C, once with LiCl Wash buffer (10mM Tris-HCl pH 8.0, 250mM LiCl, 0.5% NP-40, 0.5% DOC, 1mM EDTA pH 8.0) for 30 minutes at 4°C and once with TE buffer (1mM EDTA pH 8.0, 10mM Tris-HCl pH 8.0) for 4 minutes at 4°C. Beads were eluted with ChIP Elution buffer (50mM Tris-HCl pH 8.0, 10mM EDTA pH 8.0, 1% SDS, 1mM DTT, 50mM NaCl, 4U/ml Proteinase K (NEB), 50 μg/ml RNase A (Thermo Fisher Scientific)) at 37°C for 2 hours and de-crosslinked at 65°C overnight. Finally, DNA was purified by QIAquick PCR Purification Kit (QIAGEN) and quantified by real-time qPCR. Primers for *tim* E-box were described previously[83]. The average of ChIP signals for two intergenic regions, one on chromosome 2R (see Key Resources Table) and one on the X chromosome[83], was used for non-specific background deduction. Three technical qPCR replicates were performed for each biological ChIP replicate. Four biological ChIP replicates were performed.

QUANTIFICATION AND STATISTICAL ANALYSIS

RAIN, DODR, Rayleigh test, Shapiro-Wilk normality test and Watson Williams test were performed in R[62,63,93]. Other statistical analyses were performed using GraphPad Prism 8.0 (GraphPad Software, La Jolla, California). In the case of normally distributed data (Shapiro-Wilk normality test, $p > 0.05$), ANOVA was performed if more than two groups were compared; two-tailed Student's t test were performed if only two groups were compared. If data were not normally distributed, non-parametric Kruskall-Wallis test was applied. Asterisks indicate significant differences in mean values between genotypes or conditions at indicated time-points.

Supplementary Material

Refer to Web version on PubMed Central for supplementary material.

ACKNOWLEDGMENTS

We thank Patrick Emery for providing *p{tim(WT)-luc}* transgene, α-PER, and α-TIM antibodies for immunofluorescence; Steven Reppert and Christine Merlin for providing *Danaus plexippus* DpN1 cell line and pBA-*dpper*-FLAG plasmid; and Carrie Partch for pHis::Parallel1 plasmid for protein expression. We thank Chris Fraser and Nancy Villa for their technical help on CLOCK antigen production. We thank the Bloomington *Drosophila* Stock Center and Vienna *Drosophila* Resource Center for providing fly stocks and the Developmental Studies Hybridoma Bank for supplying α-PDF. The Confocal Microscopy facility was supported by NIH GM122968 to Pamela C. Ronald at UC Davis. Research in the laboratory of J.C.C. is supported by NIH R01 GM102225, NIH R01 DK124068, and NSF IOS 1456297.

REFERENCES

1. Dubowy C, and Sehgal A (2017). Circadian rhythms and sleep in Drosophila melanogaster. Genetics 205, 1373–1397. [PubMed: 28360128]
2. Dunlap JC, and Loros JJ (2017). Making time: conservation of biological clocks from fungi to animals. Microbiol. Spectr 5, 10.1128/microbiolspec.FUNK-0039-2016.
3. Patke A, Young MW, and Axelrod S (2020). Molecular mechanisms and physiological importance of circadian rhythms. Nat. Rev. Mol. Cell Biol 21, 67–84. [PubMed: 31768006]
4. Cox KH, and Takahashi JS (2019). Circadian clock genes and the transcriptional architecture of the clock mechanism. J. Mol. Endocrinol 63, R93–R102. [PubMed: 31557726]

5. Abruzzi KC, Rodriguez J, Menet JS, Desrochers J, Zadina A, Luo W, Tkachev S, and Rosbash M (2011). Drosophila CLOCK target gene characterization: implications for circadian tissue-specific gene expression. Genes Dev. 25, 2374–2386. [PubMed: 22085964]
6. Price JL, Blau J, Rothenfluh A, Abodeely M, Kloss B, and Young MW (1998). double-time is a novel Drosophila clock gene that regulates PERIOD protein accumulation. Cell 94, 83–95. [PubMed: 9674430]
7. Grima B, Dognon A, Lamouroux A, Chélot E, and Rouyer F (2012). CULLIN-3 controls TIMELESS oscillations in the Drosophila circadian clock. PLoS Biol. 10, e1001367. [PubMed: 22879814]
8. Zhang Y, Ling J, Yuan C, Dubruille R, and Emery P (2013). A role for Drosophila ATX2 in activation of PER translation and circadian behavior. Science 340, 879–882. [PubMed: 23687048]
9. Shakhmantsir I, Nayak S, Grant GR, and Sehgal A (2018). Spliceosome factors target timeless (*tim*) mRNA to control clock protein accumulation and circadian behavior in Drosophila. eLife 7, e39821. [PubMed: 30516472]
10. Grima B, Papin C, Martin B, Chélot E, Ponien P, Jacquet E, and Rouyer F (2019). PERIOD-controlled deadenylation of the *timeless* transcript in the *Drosophila* circadian clock. Proc. Natl. Acad. Sci. USA 116, 5721–5726. [PubMed: 30833404]
11. Saez L, and Young MW (1996). Regulation of nuclear entry of the *Drosophila* clock proteins period and timeless. Neuron 17, 911–920. [PubMed: 8938123]
12. Jang AR, Moravcevic K, Saez L, Young MW, and Sehgal A (2015). *Drosophila* TIM binds importin α1, and acts as an adapter to transport PER to the nucleus. PLoS Genet. 11, e1004974. [PubMed: 25674790]
13. Grima B, Lamouroux A, Chélot E, Papin C, Limbourg-Bouchon B, and Rouyer F (2002). The F-box protein *slimb* controls the levels of clock proteins period and timeless. Nature 420, 178–182. [PubMed: 12432393]
14. Ko HW, Jiang J, and Edery I (2002). Role for Slimb in the degradation of *Drosophila* Period protein phosphorylated by Doubletime. Nature 420, 673–678. [PubMed: 12442174]
15. Yu W, Zheng H, Houl JH, Dauwalder B, and Hardin PE (2006). PER-dependent rhythms in CLK phosphorylation and E-box binding regulate circadian transcription. Genes Dev. 20, 723–733. [PubMed: 16543224]
16. Menet JS, Abruzzi KC, Desrochers J, Rodriguez J, and Rosbash M (2010). Dynamic PER repression mechanisms in the *Drosophila* circadian clock: from on-DNA to off-DNA. Genes Dev. 24, 358–367. [PubMed: 20159956]
17. Zhou J, Yu W, and Hardin PE (2016). CLOCKWORK ORANGE enhances PERIOD mediated rhythms in transcriptional repression by antagonizing E-box binding by CLOCK-CYCLE. PLoS Genet. 12, e1006430. [PubMed: 27814361]
18. Rothenfluh A, Young MW, and Saez L (2000). ATIMELESS-independent function for PERIOD proteins in the *Drosophila* clock. Neuron 26, 505–514. [PubMed: 10839368]
19. Ashmore LJ, Sathyanarayanan S, Silvestre DW, Emerson MM, Schotland P, and Sehgal A (2003). Novel insights into the regulation of the *timeless* protein. J. Neurosci 23, 7810–7819. [PubMed: 12944510]
20. Cyran SA, Yiannoulos G, Buchsbaum AM, Saez L, Young MW, and Blau J (2005). The double-time protein kinase regulates the subcellular localization of the *Drosophila* clock protein period. J. Neurosci 25, 5430–5437. [PubMed: 15930393]
21. Vosshall LB, Price JL, Sehgal A, Saez L, and Young MW (1994). Block in nuclear localization of period protein by a second clock mutation, timeless. Science 263, 1606–1609. [PubMed: 8128247]
22. Hara T, Koh K, Combs DJ, and Sehgal A (2011). Post-translational regulation and nuclear entry of TIMELESS and PERIOD are affected in new timeless mutant. J. Neurosci 31, 9982–9990. [PubMed: 21734289]
23. Saez L, Derasmo M, Meyer P, Stieglitz J, and Young MW (2011). A key temporal delay in the circadian cycle of *Drosophila* is mediated by a nuclear localization signal in the *timeless* protein. Genetics 188, 591–600. [PubMed: 21515571]

24. Lam VH, Li YH, Liu X, Murphy KA, Diehl JS, Kwok RS, and Chiu JC (2018). CK1α collaborates with DOUBLETIME to regulate PERIOD function in the *Drosophila* circadian clock. J. Neurosci 38, 10631–10643. [PubMed: 30373768]
25. Martinek S, Inonog S, Manoukian AS, and Young MW (2001). A role for the segment polarity gene *shaggy/GSK-3* in the *Drosophila* circadian clock. Cell 105, 769–779. [PubMed: 11440719]
26. Lin JM, Kilman VL, Keegan K, Paddock B, Emery-Le M, Rosbash M, and Allada R (2002). A role for casein kinase 2α in the *Drosophila* circadian clock. Nature 420, 816–820. [PubMed: 12447397]
27. Akten B, Jauch E, Genova GK, Kim EY, Edery I, Raabe T, and Jackson FR (2003). A role for CK2 in the *Drosophila* circadian oscillator. Nat. Neurosci 6, 251–257. [PubMed: 12563262]
28. Lin JM, Schroeder A, and Allada R (2005). *In vivo* circadian function of casein kinase 2 phosphorylation sites in *Drosophila* PERIOD. J. Neurosci 25,11175–11183. [PubMed: 16319317]
29. Ko HW, Kim EY, Chiu J, Vanselow JT, Kramer A, and Edery I (2010). A hierarchical phosphorylation cascade that regulates the timing of PERIOD nuclear entry reveals novel roles for proline-directed kinases and GSK-3β/SGG in circadian clocks. J. Neurosci 30, 12664–12675. [PubMed: 20861372]
30. Meissner RA, Kilman VL, Lin JM, and Allada R (2008). TIMELESS is an important mediator of CK2 effects on circadian clock function *in vivo*. J. Neurosci 28, 9732–9740. [PubMed: 18815259]
31. Top D, Harms E, Syed S, Adams EL, and Saez L (2016). GSK-3 and CK2 kinases converge on Timeless to regulate the master clock. Cell Rep. 16, 357–367. [PubMed: 27346344]
32. Sathyanarayanan S, Zheng X, Xiao R, and Sehgal A (2004). Posttranslational regulation of Drosophila PERIOD protein by protein phosphatase 2A. Cell 116, 603–615. [PubMed: 14980226]
33. Fang Y, Sathyanarayanan S, and Sehgal A (2007). Post-translational regulation of the *Drosophila* circadian clock requires protein phosphatase 1 (PP1). Genes Dev. 21, 1506–1518. [PubMed: 17575052]
34. Myers MP, Wager-Smith K, Rothenfluh-Hilfiker A, and Young MW (1996). Light-induced degradation of TIMELESS and entrainment of the *Drosophila* circadian clock. Science 271, 1736–1740. [PubMed: 8596937]
35. Zeng H, Qian Z, Myers MP, and Rosbash M (1996). A light-entrainment mechanism for the *Drosophila* circadian clock. Nature 380,129–135. [PubMed: 8600384]
36. Ozturk N, Selby CP, Annayev Y, Zhong D, and Sancar A (2011). Reaction mechanism of *Drosophila cryptochrome*. Proc. Natl. Acad. Sci. USA 108,516–521. [PubMed: 21187431]
37. Vaidya AT, Top D, Manahan CC, Tokuda JM, Zhang S, Pollack L, Young MW, and Crane BR (2013). Flavin reduction activates *Drosophila cryptochrome*. Proc. Natl. Acad. Sci. USA 110, 20455–20460. [PubMed: 24297896]
38. Koh K, Zheng X, and Sehgal A (2006). JETLAG resets the *Drosophila* circadian clock by promoting light-induced degradation of TIMELESS. Science 312, 1809–1812. [PubMed: 16794082]
39. Peschel N, Chen KF, Szabó G, and Stanewsky R (2009). Light-dependent interactions between the *Drosophila* circadian clock factors *cryptochrome*, *jetlag*, and *timeless*. Curr. Biol 19, 241–247. [PubMed: 19185492]
40. Naidoo N, Song W, Hunter-Ensor M, and Sehgal A (1999). A role for the proteasome in the light response of the timeless clock protein. Science 285, 1737–1741. [PubMed: 10481010]
41. Chiu JC, Vanselow JT, Kramer A, and Edery I (2008). The phospho-occupancy of an atypical SLIMB-binding site on PERIOD that is phosphorylated by DOUBLETIME controls the pace of the clock. Genes Dev. 22, 1758–1772. [PubMed: 18593878]
42. Chiu JC, Ko HW, and Edery I (2011). NEMO/NLK phosphorylates PERIOD to initiate a time-delay phosphorylation circuit that sets circadian clock speed. Cell 145, 357–370. [PubMed: 21514639]
43. Garbe DS, Fang Y, Zheng X, Sowcik M, Anjum R, Gygi SP, and Sehgal A (2013). Cooperative interaction between phosphorylation sites on PERIOD maintains circadian period in *Drosophila*. PLoS Genet. 9, e1003749. [PubMed: 24086144]

44. Yildirim E, Chiu JC, and Edery I (2015). Identification of light-sensitive phosphorylation sites on PERIOD that regulate the pace of circadian rhythms in *Drosophila*. Mol. Cell. Biol 36, 855–870. [PubMed: 26711257]
45. Top D, O'Neil JL, Merz GE, Dusad K, Crane BR, and Young MW (2018). CK1/Doubletime activity delays transcription activation in the circadian clock. eLife 7, e32679. [PubMed: 29611807]
46. Singh S, Giesecke A, Damulewicz M, Fexova S, Mazzotta GM, Stanewsky R, and Dolezel D (2019). New *Drosophila* circadian clock mutants affecting temperature compensation induced by targeted mutagenesis of *Timeless*. Front. Physiol 10, 1442. [PubMed: 31849700]
47. Li YH, Liu X, Vanselow JT, Zheng H, Schlosser A, and Chiu JC (2019). O-GlcNAcylation of PERIOD regulates its interaction with CLOCK and timing of circadian transcriptional repression. PLoS Genet. 15, e1007953. [PubMed: 30703153]
48. Kaasik K, Kivimäe S, Allen JJ, Chalkley RJ, Huang Y, Baer K, Kissel H, Burlingame AL, Shokat KM, Ptáček LJ, and Fu YH (2013). Glucose sensor O-GlcNAcylation coordinates with phosphorylation to regulate circadian clock. Cell Metab. 17, 291–302. [PubMed: 23395175]
49. Kim EY, Jeong EH, Park S, Jeong HJ, Edery I, and Cho JW (2012). A role for O-GlcNAcylation in setting circadian clock speed. Genes Dev. 26, 490–502. [PubMed: 22327476]
50. Ousley A, Zafarullah K, Chen Y, Emerson M, Hickman L, and Sehgal A (1998). Conserved regions of the *timeless* (*tim*) clock gene in *Drosophila* analyzed through phylogenetic and functional studies. Genetics 148, 815–825. [PubMed: 9504927]
51. Sehgal A, Rothenfluh-Hilfiker A, Hunter-Ensor M, Chen Y, Myers MP, and Young MW (1995). Rhythmic expression of *timeless*: a basis for promoting circadian cycles in *period* gene autoregulation. Science 270, 808–810. [PubMed: 7481772]
52. Tauber E, Zordan M, Sandrelli F, Pegoraro M, Osterwalder N, Breda C, Daga A, Selmin A, Monger K, Benna C, et al. (2007). Natural selection favors a newly derived *timeless* allele in *Drosophila melanogaster*. Science 316, 1895–1898. [PubMed: 17600215]
53. Myers MP, Wager-Smith K, Wesley CS, Young MW, and Sehgal A (1995). Positional cloning and sequence analysis of the Drosophila clock gene, timeless. Science 270, 805–808. [PubMed: 7481771]
54. Yang Z, Emerson M, Su HS, and Sehgal A (1998). Response of the timeless protein to light correlates with behavioral entrainment and suggests a nonvisual pathway for circadian photoreception. Neuron 21, 215–223. [PubMed: 9697865]
55. Shafer OT, Rosbash M, and Truman JW (2002). Sequential nuclear accumulation of the clock proteins period and *timeless* in the pacemaker neurons of *Drosophila melanogaster*. J. Neurosci 22, 5946–5954. [PubMed: 12122057]
56. Muskus MJ, Preuss F, Fan JY, Bjes ES, and Price JL (2007). *Drosophila* DBT lacking protein kinase activity produces long-period and arrhythmic circadian behavioral and molecular rhythms. Mol. Cell. Biol 27, 8049–8064. [PubMed: 17893330]
57. Nardozzi JD, Lott K, and Cingolani G (2010). Phosphorylation meets nuclear import: a review. Cell Commun. Signal. 8, 32. [PubMed: 21182795]
58. Fung HY, Fu SC, and Chook YM (2017). Nuclear export receptor CRM1 recognizes diverse conformations in nuclear export signals. eLife 6, e23961. [PubMed: 28282025]
59. Alt JR, Cleveland JL, Hannink M, and Diehl JA (2000). Phosphorylation-dependent regulation of cyclin D1 nuclear export and cyclin D1-dependent cellular transformation. Genes Dev. 14, 3102–3114. [PubMed: 11124803]
60. Napolitano G, Esposito A, Choi H, Matarese M, Benedetti V, Di Malta C, Monfregola J, Medina DL, Lippincott-Schwartz J, and Ballabio A (2018). mTOR-dependent phosphorylation controls TFEB nuclear export. Nat. Commun 9, 3312. [PubMed: 30120233]
61. Edery I, Zwiebel LJ, Dembinska ME, and Rosbash M (1994). Temporal phosphorylation of the *Drosophila period* protein. Proc. Natl. Acad. Sci. USA 91, 2260–2264. [PubMed: 8134384]
62. Thaben PF, and Westermark PO (2016). Differential rhythmicity: detecting altered rhythmicity in biological data. Bioinformatics 32, 2800–2808. [PubMed: 27207944]
63. Thaben PF, and Westermark PO (2014). Detecting rhythms in time series with RAIN. J. Biol. Rhythms 29, 391–400. [PubMed: 25326247]

64. Kim EY, Ko HW, Yu W, Hardin PE, and Edery I (2007). A DOUBLETIME kinase binding domain on the *Drosophila* PERIOD protein is essential for its hyperphosphorylation, transcriptional repression, and circadian clock function. Mol. Cell. Biol 27, 5014–5028. [PubMed: 17452449]

65. Hung HC, Maurer C, Zorn D, Chang WL, and Weber F (2009). Sequential and compartment-specific phosphorylation controls the life cycle of the circadian CLOCK protein. J. Biol. Chem 284, 23734–23742. [PubMed: 19564332]

66. Yu W, Houl JH, and Hardin PE (2011). NEMO kinase contributes to core period determination by slowing the pace of the *Drosophila* circadian oscillator. Curr. Biol 21, 756–761. [PubMed: 21514156]

67. Szabó A, Papin C, Zorn D, Ponien P, Weber F, Raabe T, and Rouyer F (2013). The CK2 kinase stabilizes CLOCK and represses its activity in the *Drosophila* circadian oscillator. PLoS Biol. 11, e1001645. [PubMed: 24013921]

68. Mahesh G, Jeong E, Ng FS, Liu Y, Gunawardhana K, Houl JH, Yildirim E, Amunugama R, Jones R, Allen DL, et al. (2014). Phosphorylation of the transcription activator CLOCK regulates progression through a ~ 24-h feedback loop to influence the circadian period in Drosophila. J. Biol. Chem 289, 19681–19693. [PubMed: 24872414]

69. Yu W, Zheng H, Price JL, and Hardin PE (2009). DOUBLETIME plays a noncatalytic role to mediate CLOCK phosphorylation and repress CLOCK-dependent transcription within the *Drosophila* circadian clock. Mol. Cell. Biol 29, 1452–1458. [PubMed: 19139270]

70. Andreazza S, Bouleau S, Martin B, Lamouroux A, Ponien P, Papin C, Chélot E, Jacquet E, and Rouyer F (2015). Daytime CLOCK dephosphorylation is controlled by STRIPAK complexes in *Drosophila*. Cell Rep. 11, 1266–1279. [PubMed: 25981041]

71. Wong YH, Lee TY, Liang HK, Huang CM, Wang TY, Yang YH, Chu CH, Huang HD, Ko MT, and Hwang JK (2007). KinasePhos 2.0: a web server for identifying protein kinase-specific phosphorylation sites based on sequences and coupling patterns. Nucleic Acids Res. 35, W588–W594. [PubMed: 17517770]

72. Blau J, and Young MW (1999). Cycling *vrille* expression is required for a functional *Drosophila* clock. Cell 99, 661–671. [PubMed: 10612401]

73. Luo W, Li Y, Tang CH, Abruzzi KC, Rodriguez J, Pescatore S, and Rosbash M (2012). CLOCK deubiquitylation by USP8 inhibits CLK/CYC transcription in *Drosophila*. Genes Dev. 26, 2536–2549. [PubMed: 23154984]

74. Yagita K, Tamanini F, Yasuda M, Hoeijmakers JH, van der Horst GT, and Okamura H (2002). Nucleocytoplasmic shuttling and mCRY-dependent inhibition of ubiquitylation of the mPER2 clock protein. EMBO J. 21, 1301–1314. [PubMed: 11889036]

75. Diernfellner AC, Querfurth C, Salazar C, Höfer T, and Brunner M (2009). Phosphorylation modulates rapid nucleocytoplasmic shuttling and cytoplasmic accumulation of *Neurospora* clock protein FRQ on a circadian time scale. Genes Dev. 23, 2192–2200. [PubMed: 19759264]

76. Öllinger R, Korge S, Korte T, Koller B, Herrmann A, and Kramer A (2014). Dynamics of the circadian clock protein PERIOD2 in living cells. J. Cell Sci 127, 4322–4328. [PubMed: 25074809]

77. Tanaka M, Ichinose S, Shintani T, and Gomi K (2018). Nuclear export-dependent degradation of the carbon catabolite repressor CreA is regulated by a region located near the C-terminus in *Aspergillus oryzae*. Mol. Microbiol 110, 176–190. [PubMed: 29995996]

78. Markiewicz Ł, Uśpieński T, Niedziółka SM, and Niewiadomski P (2020). Xpo7 negatively regulates Hedgehog signaling by exporting Gli2 from the nucleus. bioRxiv. 10.1101/2020.01.31.928408.

79. Benna C, Bonaccorsi S, Wülbeck C, Helfrich-Förster C, Gatti M, Kyriacou CP, Costa R, and Sandrelli F (2010). *Drosophila timeless2* is required for chromosome stability and circadian photoreception. Curr. Biol 20, 346–352. [PubMed: 20153199]

80. Lam VH, and Chiu JC (2017). Evolution and design of invertebrate circadian clocks In Oxford Handbook of Invertebrate Neurobiology, Byrne JH, ed. (Oxford University), pp. 595–614.

81. Kurien P, Hsu PK, Leon J, Wu D, McMahon T, Shi G, Xu Y, Lipzen A, Pennacchio LA, Jones CR, et al. (2019). TIMELESS mutation alters phase responsiveness and causes advanced sleep phase. Proc. Natl. Acad. Sci. USA 116, 12045–12053. [PubMed: 31138685]

82. Abrieux A, Xue Y, Cai Y, Lewald KM, Nguyen HN, Zhang Y, and Chiu JC (2020). EYES ABSENT and TIMELESS integrate photoperiodic and temperature cues to regulate seasonal physiology in *Drosophila*. Proc. Natl. Acad. Sci. USA 117, 15293–15304. [PubMed: 32541062]

83. Kwok RS, Li YH, Lei AJ, Edery I, and Chiu JC (2015). The catalytic and non-catalytic functions of the Brahma chromatin-remodeling protein collaborate to fine-tune circadian transcription in *Drosophila*. PLoS Genet. 11, e1005307. [PubMed: 26132408]

84. Rakshit K, Krishnan N, Guzik EM, Pyza E, and Giebultowicz JM (2012). Effects of aging on the molecular circadian oscillations in *Drosophila*. Chronobiol. Int 29, 5–14. [PubMed: 22217096]

85. Zhu H, Sauman I, Yuan Q, Casselman A, Emery-Le M, Emery P, and Reppert SM (2008). Cryptochromes define a novel circadian clock mechanism in monarch butterflies that may underlie sun compass navigation. PLoS Biol. 6, e4.

86. Fraser CS, Berry KE, Hershey JW, and Doudna JA (2007). eIF3j is located in the decoding center of the human 40S ribosomal subunit. Mol. Cell 26,811–819. [PubMed: 17588516]

87. Gustafson CL, Parsley NC, Asimgil H, Lee HW, Ahlbach C, Michael AK, Xu H, Williams OL, Davis TL, Liu AC, and Partch CL (2017). A slow conformational switch in the BMAL1 transactivation domain modulates circadian rhythms. Mol. Cell 66, 447–457.e7. [PubMed: 28506462]

88. Groth AC, Fish M, Nusse R, and Calos MP (2004). Construction of transgenic Drosophila by using the site-specific integrase from phage phiC31. Genetics 166, 1775–1782. [PubMed: 15126397]

89. Brand AH, and Perrimon N (1993). Targeted gene expression as a means of altering cell fates and generating dominant phenotypes. Development 118, 401–415. [PubMed: 8223268]

90. Chiu JC, Low KH, Pike DH, Yildirim E, and Edery I (2010).Assaying locomotor activity to study circadian rhythms and sleep parameters in *Drosophila*. J. Vis. Exp 43, 2157.

91. Xue Y, Chiu JC, and Zhang Y (2019). SUR-8 interacts with PP1-87B to stabilize PERIOD and regulate circadian rhythms in *Drosophila*. PLoS Genet. 15, e1008475. [PubMed: 31710605]

92. Schindelin J, Arganda-Carreras I, Frise E, Kaynig V, Longair M, Pietzsch T, Preibisch S, Rueden C, Saalfeld S, Schmid B, et al. (2012). Fiji: an open-source platform for biological-image analysis. Nat. Methods 9, 676–682. [PubMed: 22743772]

93. Batschelet E (1981). Circular Statistics in Biology (Academic).

Highlights

- Twelve phosphorylation sites were identified in PER-bound TIM protein
- Abolishing phosphorylation of conserved TIM(S1404) alters circadian rhythms
- CK2 phosphorylates S1404 to inhibit interaction of TIM and nuclear export complex
- PER-TIM nuclear accumulation regulates the timing of CLK transcriptional activity

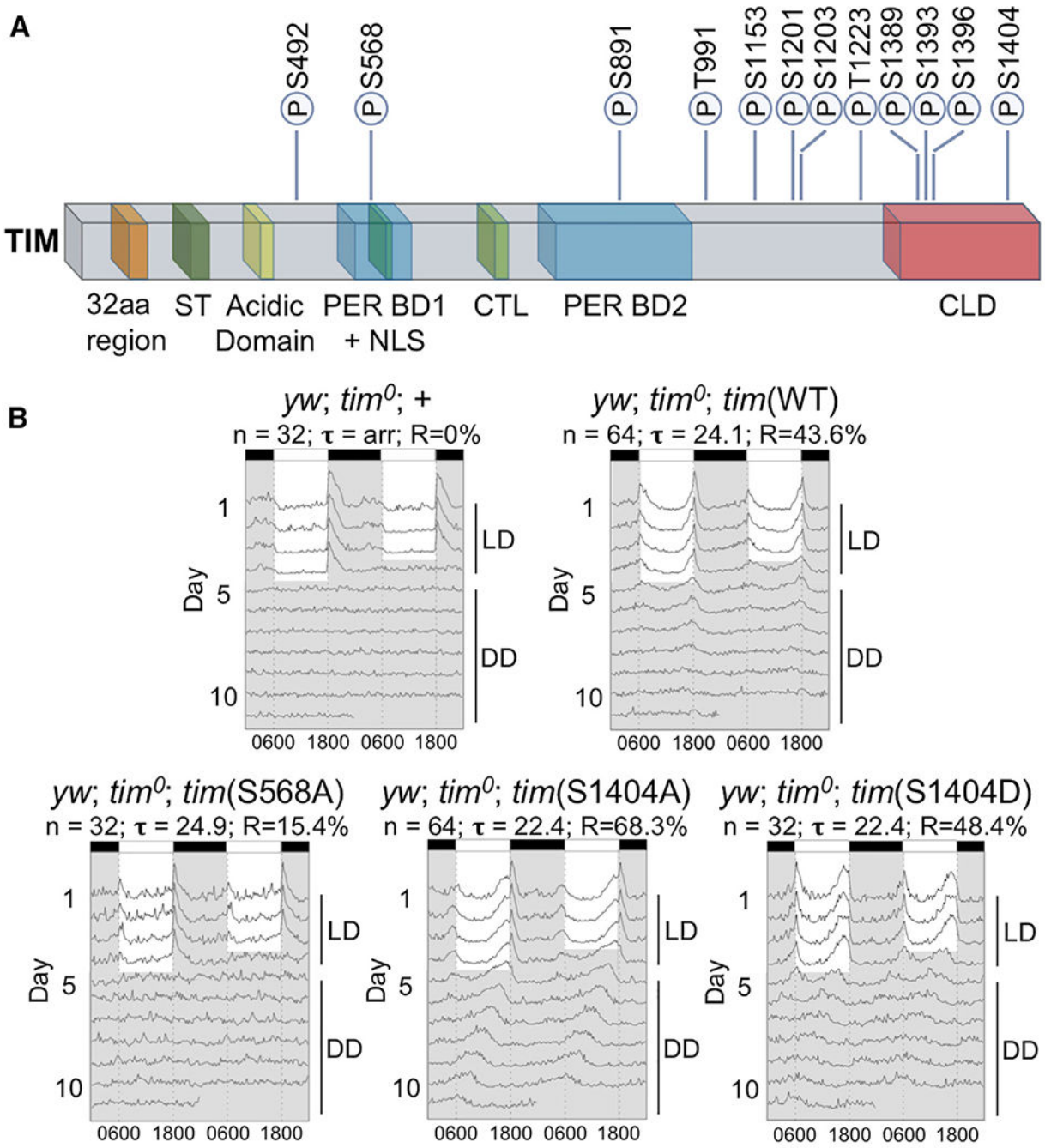

Figure 1. Daily Locomotor Activity Rhythms Are Altered in TIM Phosphorylation Site Mutants

(A) Schematic showing phosphorylation sites mapped onto TIM functional domains. All amino acid numbering is based on the L-TIM$_{1421}$ isoform.[50,51,52] Previously described domains of TIM: 32 amino acid region (amino acids [aas] 260–291),[50] also known as serine-rich domain (SRD) (aas 260–292);[30] serine/threonine (ST)-rich region (aas 293–312);[31] acidic domain (aas 383–412);[52] PER binding domain 1 (PER BD1) (aas 536–610);[11] nuclear localization sequence (NLS) (aas 558–583);[11] C-terminal tail-like sequence (CTL) (aas 640–649);[37] PER binding domain 2 (PER BD2) (aas 747–946);[11] and cytoplasmic localization

domain (CLD) (aas 1,261–1,421).[11] Corresponding PEAKS Studio scores of modified peptides are shown in Table S1.

(B) Double-plotted actograms of *yw*; *tim*^{0} flies carrying transgenes for site-specific TIM phosphorylation mutations generated using FaasX. Average activity of each genotype was plotted. n represents the sample size for behavioral assay. Tau (τ) represents the average period length of the indicated group of flies in DD (SEM is shown in Table S2). R represents percentage of flies that are rhythmic. Flies were entrained for 4 days in LD and then switched to 7 days of constant darkness (DD).

See also Figures S1 and S2 and Tables S1 and S2.

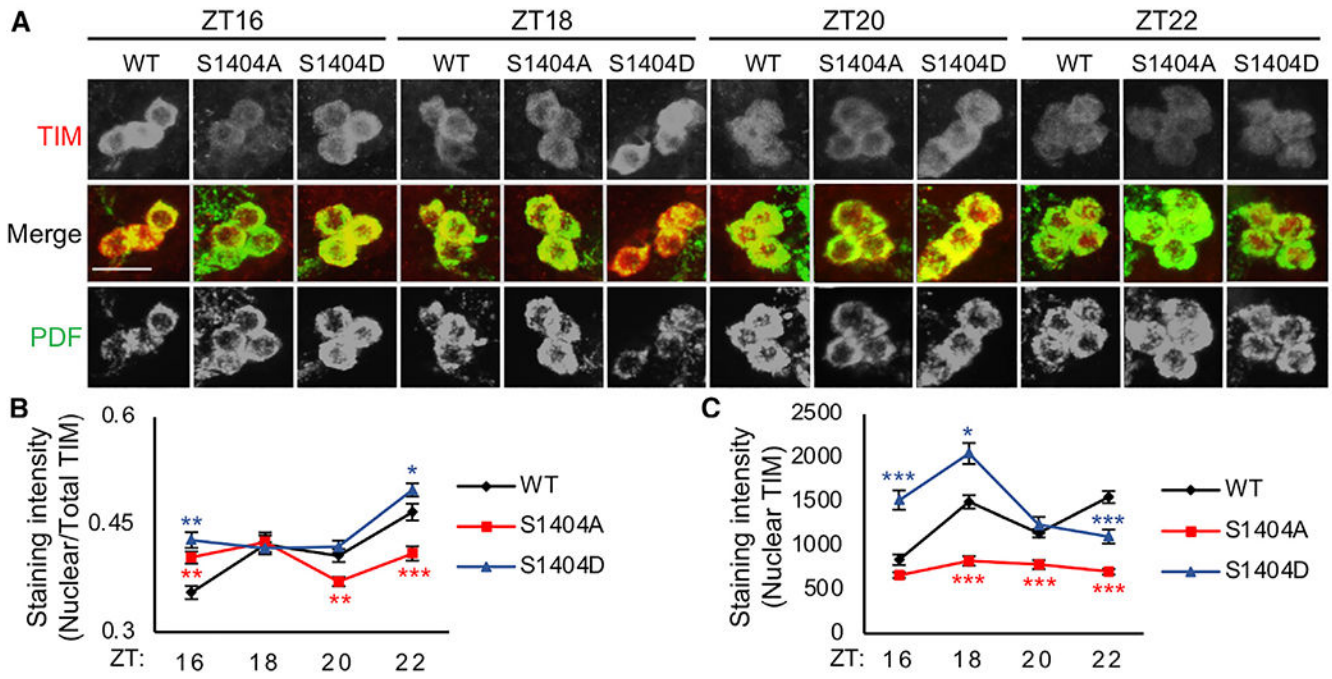

Figure 2. TIM Nuclear Accumulation Is Altered in *tim*(S1404A) and *tim*(S1404D) Mutants

(A) Representative confocal images of sLN_vs clock neurons in adult fly brains stained with α-TIM (red) and α-PDF (green). Single channels are shown in gray scale. Scale bar (merged image in WT ZT16) represents 10 μm. Flies were entrained for 4 days in LD cycles and collected at the indicated times on LD4 for fixation and immunofluorescence analysis.

(B) Line graph showing the fraction of nuclear TIM presented as nuclear TIM divided by total TIM in sLN_vs.

(C) Line graph showing nuclear TIM staining intensity in sLN_vs.

Error bars indicate SEM (n > 30); ***p < 0.001; **p < 0.01; *p < 0.05; Kruskal-Wallis test.

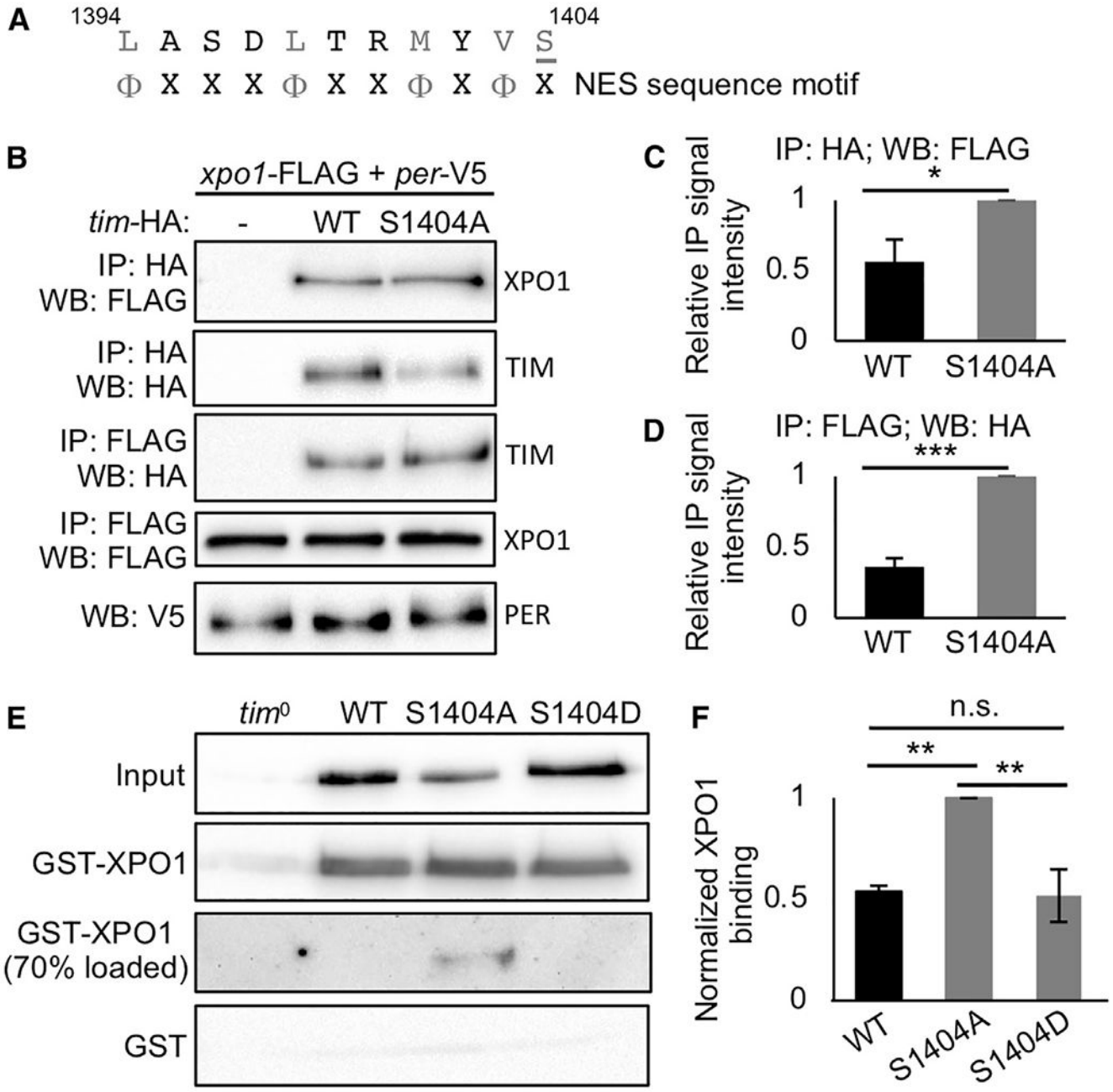

Figure 3. TIM(S1404) Phosphorylation Promotes TIM Nuclear Retention by Compromising TIM-XPO1 Interaction

(A) S1404 is located next to a putative TIM^{NES}: L1394-V1403. S1404 is underlined and shown in gray. Classical NES sequence motif is previously investigated.[58] Φ is hydrophobic amino acid (in gray): Leu; Val; Ile; Phe; or Met. X is any amino acid.

(B) Western blots showing reciprocal coimmunoprecipitations (coIPs) to examine the interactions of TIM(WT) or TIM(S1404A) to XPO1 in *Drosophila* S2 cells expressing pAc-*xpo1*-3XFLAG-6XHIS and pAc-*per*-V5 in the presence or absence of pAc-HA plasmids expressing *tim* variants. Protein extracts were directly analyzed by immunoblotting (α-V5

for PER) or immunoprecipitated with α-HA or α-FLAG resins to detect baits and interactors.

(C and D) Bar graphs displaying quantification of reciprocal coIPs. Values for binding are normalized to amount of bait detected in the IPs and expressed as relative signal intensity (high value = 1). Error bars indicate ± SEM (n = 4); ***p < 0.001; *p < 0.05; two-tailed Student's t test.

(E) Western blots showing GST-XPO1 pull-down of fly head extracts. Flies were entrained in LD cycles and collected on LD3 at ZT20. The relative amount of TIM (input) from four genotypes and that bound to GST-XPO1 or GST-bound glutathione resins were shown. To highlight the difference between genotypes, reduced amount (70%) of GST-XPO1 pull-down reactions were loaded (third panel from top).

(F) Bar graphs displaying quantification of TIM from GST-XPO1 pull-down in (E). TIMs bound to GST-XPO1 were normalized to input and expressed as relative signal intensity (high value = 1). Error bars indicate ± SEM (n = 3); **p < 0.01; one-way ANOVA.

See also Figures S3 and S4.

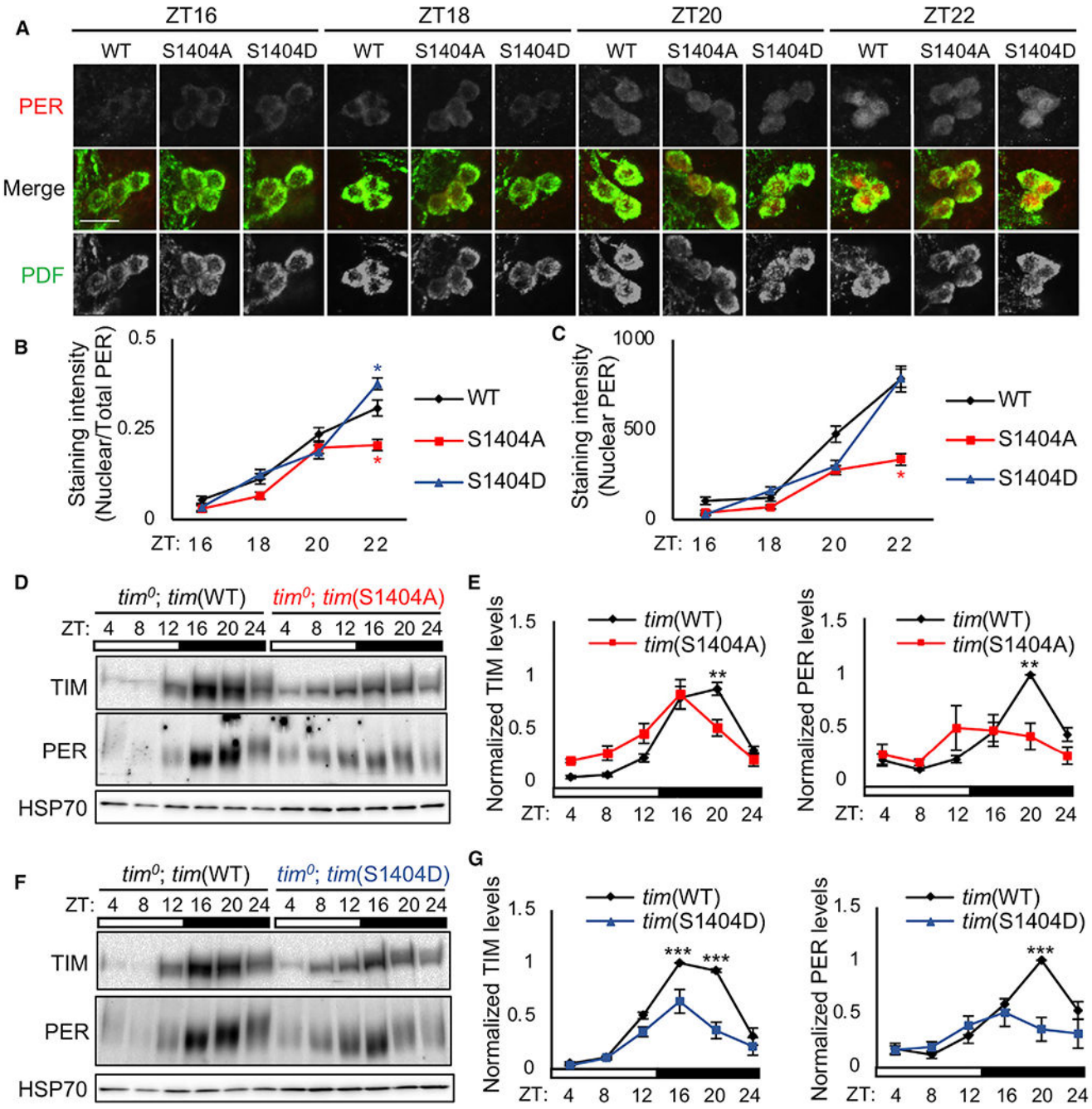

Figure 4. Altered TIM(S1404) Phosphorylation Influences PER Nuclear Accumulation

(A) Representative confocal images of sLN_v clock neurons in adult fly brains stained with α-PER (red) and α-PDF (green). Single channels are shown in gray scale. Scale bar (merged image in WT ZT16) represents 10 μm. Flies were entrained as described in Figure 2A.

(B) Line graph showing the fraction of nuclear PER in sLN_vs presented as nuclear PER divided by total PER.

(C) Line graph showing nuclear PER staining intensity in sLN_vs. Error bars indicate ± SEM ($n > 27$); *$p < 0.05$; Kruskal-Wallis test.

(D and F) Western blots comparing TIM and PER profiles in heads of (D) *tim*(WT) and *tim*(S1404A) flies or (F) *tim*(WT) and *tim*(S1404D) flies. Flies were entrained in LD cycles and collected on LD3 at indicated time points (ZT). α-HSP70 was used to indicate equal loading and for normalization.

(E and G) Quantification of TIM and PER in (D) and (F). Error bars indicate ± SEM (n = 3); ***p < 0.001; **p < 0.01; two-way ANOVA.

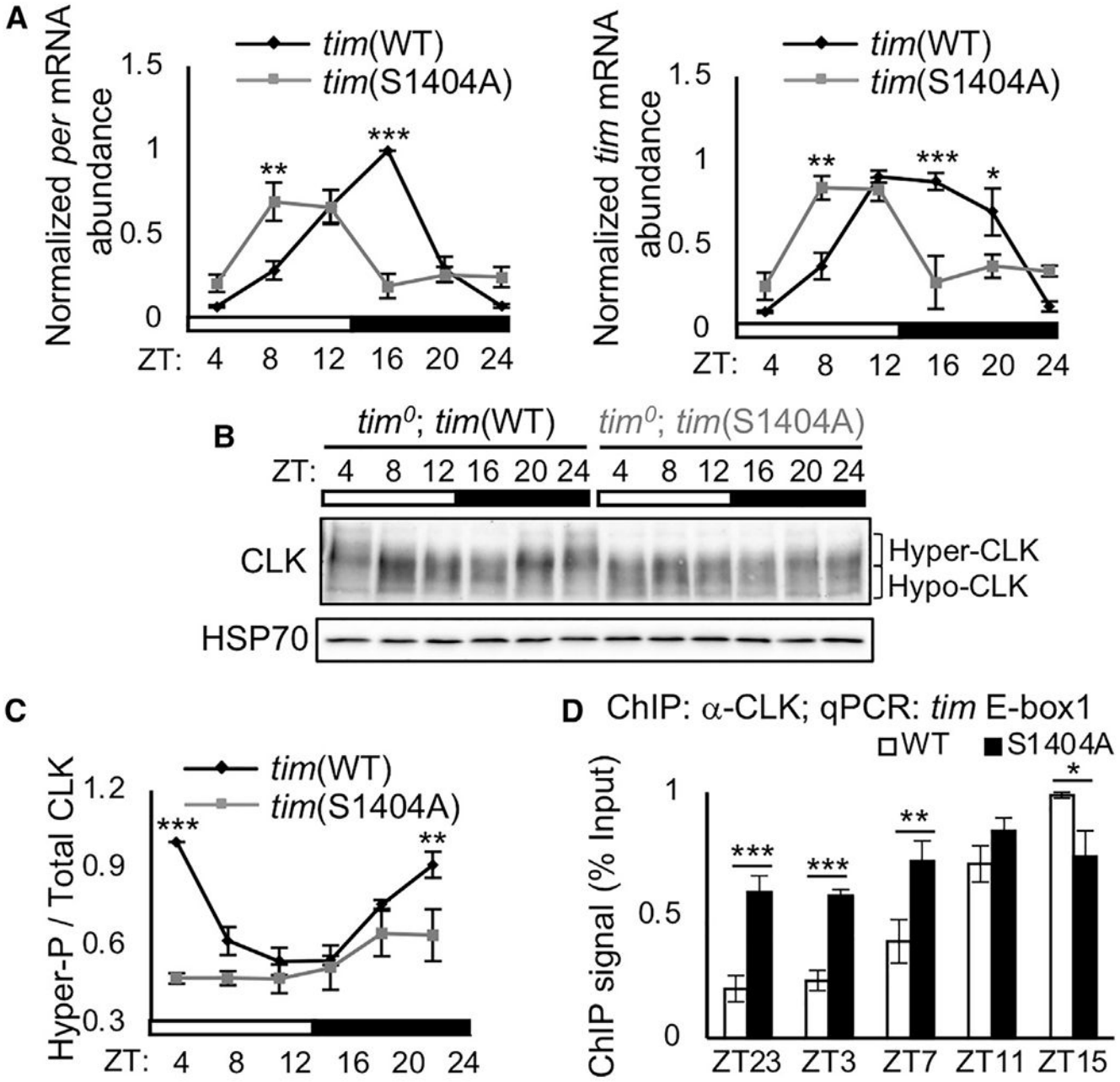

Figure 5. Reduced TIM Nuclear Retention in *tim*(S1404A) Mutant Leads to Dampening of CLK Phosphorylation Rhythm and Phase Advance in CLK-Activated Transcriptional Activation

(A) Steady-state mRNA expression of *per* and *tim* in heads of *tim*(WT) and *tim*(S1404A) flies. Flies were entrained in LD cycles and collected on LD3 at indicated time points (ZT; n = 3).

(B) Western blots comparing CLK protein profiles in heads of *tim*(WT) and *tim*(S1404A) entrained and collected as in (A). Brackets indicate hypo- and hyperphosphorylated CLK isoforms. α-HSP70 was used to indicate equal loading and for normalization.

(C) Quantification of hyperphosphorylated/total CLK. The top half of the CLK signal shown at ZT24 in *tim*(WT) flies (lane 6) is used as a reference to classify CLK isoforms as hyperphosphorylated (n = 3).

(D) ChIP assays using fly head extracts comparing CLK occupancy at *tim* promoter in *tim*(WT) and *tim*(S1404A) flies. CLK-ChIP signals were normalized to % input. ChIP signals for two intergenic regions were used for non-specific background deduction (n = 4). Error bars indicate ± SEM; ***p < 0.001; **p < 0.01; *p < 0.05; two-way ANOVA. See also Figures S5 and S6.

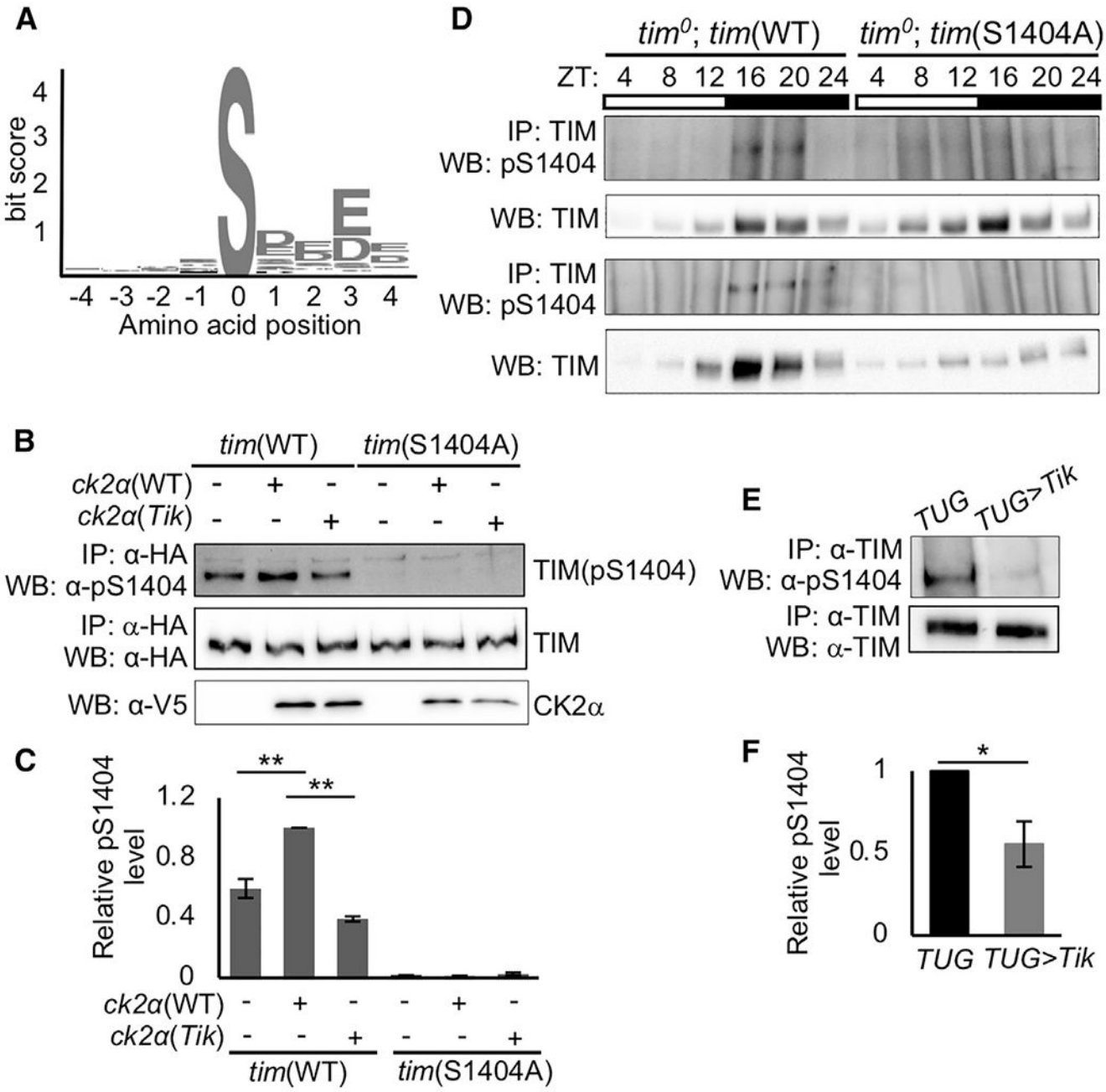

Figure 6. CK2 Phosphorylates TIM(S1404)

(A) CK2 consensus motifs generated by KinasePhos 2.0. S1404 corresponds to phosphoserine at amino acid position 0 (Support vector machine score = 0.9581).

(B) *Drosophila* S2 cells were transfected with pAc-*tim*(WT)-HA or pAc-*tim*(S1404A)-HA and co-transfected with an empty plasmid (pMT-V5-His), pMT-*ck2α*-V5, or pMT-*ck2α*(M161K E165D)-V5, referred to as *ck2α*(*tik*). Protein extracts were incubated with α-HA resin. Total TIM isoforms, TIM(pS1404), and CK2α protein levels were analyzed by western blotting with indicated antibodies.

(C) Bar graph showing relative TIM pS1404 levels in (B) normalized to total TIM isoforms. Error bars indicate ± SEM (n = 2); **p < 0.01; two-way ANOVA.
(D) Fly heads of the specified genotypes were collected at the indicated times on LD3 after 2 days of entrainment. TIM was immunoprecipitated with α-TIM prior to western blotting with α-pS1404 (top panel). Total TIM isoforms are shown in the bottom panel. 2 biological replicates are shown.
(E) Reduced pS1404 in flies overexpressing *ck2α*(*tik*) in *tim*-expressing cells (*TUG>tik*) as compared to parental control (*TUG*). Flies were entrained and collected on LD3 at ZT20. Fly head extracts were immunoprecipitated with α-TIM. TIM(pS1404) and total TIM isoforms were analyzed by western blotting.
(F) Bar graph showing relative pS1404 levels in (E), normalized to total TIM isoforms. Error bars indicate ± SEM (n = 4); *p < 0.05; two-tailed Student's t test.
See also Figure S4.

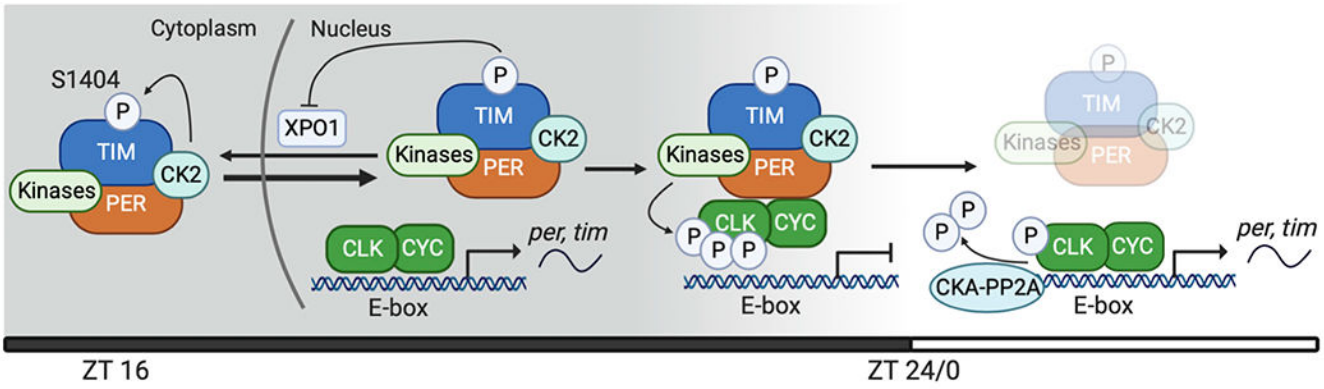

Figure 7. A Model Describing the Function of TIM(S1404) Phosphorylation in Regulating the Molecular Clock

TIM(S1404) is phosphorylated by CK2 in the cytoplasm in early night. Upon entering the nucleus, phosphorylation at S1404 inhibits interaction of TIM and XPO1 and nuclear export of PER-TIM heterodimers, thereby promoting their nuclear accumulation. This allows kinase(s) bound to PER-TIM complex to phosphorylate CLK and remove CLK from circadian promoters. The kinase(s) responsible for this step is currently unknown. CKA-PP2A then dephosphorylates CLK and promotes the onset of CLK transcriptional activity in the next cycle.[70] Other phosphorylation events on PER-TIM are not depicted for simplicity.

KEY RESOURCES TABLE

REAGENT or RESOURCE	SOURCE	IDENTIFIER
Antibodies		
Guinea pig polyclonal anti-DpPER	This paper	RRID: AB_2832970
Rat monoclonal anti-HA (clone 3F10)	Roche	Cat#12013819001
Mouse monoclonal anti-V5	Thermo Fisher Scientific	Car#R960-25
Mouse monoclonal anti-FLAG M2	Sigma-Aldrich	Cat#M3165
Goat polyclonal anti-GST	GE Healthcare	Cat#GE27-4577-01
Rat polyclonal anti-TIM (R5839)	[87]	RRID: AB_2782953
Rabbit polyclonal anti-pS1404 (RB S4602)	This paper	RRID: AB_2814716
Guinea pig polyclonal anti-CLK (GP 6139)	This paper	RRID: AB_2827523
Guinea pig polyclonal anti-PER (GP5620)	[86]	RRID: AB_2747405
Mouse monoclonal anti-HSP70 (clone BRM-22)	Sigma-Aldrich	Cat#SAB4200714
Goat anti-mouse IgG-HRP	GE Healthcare	Cat#NA931
Mouse anti-goat IgG-HRP	Santa Cruz Biotechnology	Cat#sc-2354
Goat anti-guinea pig IgG-HRP	Sigma-Aldrich	Cat#A7289
Donkey anti-rabbit IgG-HRP	GE Healthcare	Cat#NA934
Goat anti-rat IgG-HRP	GE Healthcare	Cat#NA935
Rabbit polyclonal anti-PER	[35]	N/A
Guinea pig polyclonal anti-TIM	[91]	N/A
Mouse monoclonal anti-PDF (clone C7-C)	Developmental Studies Hybridoma Bank	RRID: AB_760350 and AB_2315084
Cy3 AffiniPure donkey anti-rat IgG (H+L)	Jackson Immunoresearch	Cat#712-165-153RRID: AB_2340667
Alexa Fluor 488 AffiniPure donkey anti-rabbit-IgG (H+L)	Jackson Immunoresearch	Cat#711-545-152; RRID: AB_2313584
Cy5 AffiniPure donkey anti-mouse IgG (H+L)	Jackson Immunoresearch	Cat#715-175-150; RRID: AB_2340819
Bacterial and Virus Strains		
DH10BAC *E. coli*	Thermo Fisher Scientific	Cat#10361012
Sf9 cells	Thermo Fisher Scientific	Cat#11496015
BL21(DE3) *E. coli*	Sigma-Aldrich	Cat#70954
Chemicals, Peptides, and Recombinant Proteins		
Pfu Turbo Cx Hotstart DNA polymerase	Agilent	Cat#600410-51
Bacto Agar	BD Biosciences	Cat#90000-767
Grace's Insect Medium	Thermo Fisher Scientific	Cat#11605-094
Schneider's *Drosophila* Medium	Thermo Fisher Scientific	Cat#21720-024
Fetal Bovine Serum	VWR	Cat# 97068-085
Penicillin/streptomycin	Thermo Fisher Scientific	Cat#15-140-148
Trypsin/EDTA	Thermo Fisher Scientific	Cat#25300-062
TRI regent	Sigma-Aldrich	Cat#T9424
MG132	Sigma-Aldrich	Cat#C2211

REAGENT or RESOURCE	SOURCE	IDENTIFIER
Aprotinin	Sigma-Aldrich	Cat#A1153
Leupeptin	Sigma-Aldrich	Cat#L2884
Pepstatin A	Sigma-Aldrich	Cat#P5318
5ml IMAC Nickle column	Bio-Rad	Cat #7800811
Ni-NTA Superflow nickle-charged resin	QIAGEN	Cat#30761
SIGMAFAST™ Protease Inhibitor Cocktail, EDTA-FREE	Sigma-Aldrich	Cat#S8830
anti-HA Affinity Matrix	Sigma-Aldrich	Cat#11815016001
ANTI-FLAG M2 Affinity Gel	Sigma-Aldrich	Cat#A2220
Glutathione Sepharose 4B	GE Healthcare	Cat#GE17-0756-01
PhosSTOP	Sigma-Aldrich	Cat#4906845001
GammaBind Plus Sepharose antibody purification resin	GE Healthcare	Cat#17088601
Normal Goat Serum	Jackson Immunoresearch	Cat#005-000-121
λ-Phosphatase	NEB	Cat#P0753S
RQ1 DNase	Promega	Cat#M6101
SsoAdvanced SYBR green supermix	Bio-Rad	Cat#1725270
Peptide: DLTRMYVpSDEDDRLE; where p = phosphate	This paper	N/A
IGEPAL CA-630	Sigma-Aldrich	Cat#8896
Tergitol NP-40	Sigma-Aldrich	Cat#NP40S
Tergitol NP-10	Sigma-Aldrich	Cat#NP10
AcBSA	Promega	Cat#R3961
RNase A	Thermo Fisher Scientific	Cat#EN0531
Proteinase K	NEB	Cat#P8107S
Dynabeads Protein G	Thermo Fisher Scientific	Cat#10003D
Critical Commercial Assays		
Superscript IV	Thermo Fisher Scientific	Cat#18091050
Effectene Transfection Reagents	QIAGEN	Cat#301425
Pierce Coomassie Plus Assay Reagents	Thermo Fisher Scientific	Cat#1856210
XtremeGENE 9	Sigma-Aldrich	Cat#6365779001
QIAquick PCR Purification Kit	QIAGEN	Cat#28106
Deposited Data		
D. melanogaster MS data	This paper	Chorus repository: project ID 1424
Dannaus plexippus DpNI MS data	This paper	ProteomeXchange: MSV000085748
Experimental Models: Cell Lines		
D. melanogaster: Cell line S2: S2-DRSC	Thermo Fisher Scientific	Cat#R69007
Dannaus plexippus: Cell line DpN1	[84]	N/A
Experimental Models: Fly Lines		
D. melanogaster: w; UAS-dicer2; tim-UAS-Gal4	[69]	N/A
D. melanogaster: w; UAS-ck2^{ik}	Bloomington Drosophila Stock Center	#24624
D. melanogaster: yw; *tim*^{0}	[50]	N/A

REAGENT or RESOURCE	SOURCE	IDENTIFIER
D. melanogaster: w; *clk*^{out}	[65]	N/A
D. melanogaster: w^{1118}	Bloomington Drosophila Stock Center	B#3605
D. melanogaster: yw; tim^{0}*; tim*(WT)	This paper	N/A
D. melanogaster: yw; tim^{0}*; tim*(S492A)	This paper	N/A
D. melanogaster: yw; tim^{0}*; tim*(S568A)	This paper	N/A
D. melanogaster: yw; tim^{0}*; tim*(S891A)	This paper	N/A
D. melanogaster: yw; tim^{0}*; tim*(S1153A)	This paper	N/A
D. melanogaster: yw; tim^{0}*; tim*(T1200-1205A)	This paper	N/A
D. melanogaster: yw; tim^{0}*; tim*(S1404A)	This paper	N/A
D. melanogaster: yw; tim^{0}*; tim*(S1404D)	This paper	N/A
Oligonucleotides		
See Table S3 for primers for PCR mutagenesis, ChIP analysis and qPCR analysis.	This paper	N/A
Recombinant DNA		
Plasmid: pAc-*per*-V5-HIS	[61]	N/A
Plasmid: pAc-3XFLAG-6XHIS	[42]	
Plasmid: pAc-*xpo1*-3XFLAG-6XHIS	This paper	N/A
Plasmid: pAc-*tim*(WT)-HA	[14]	N/A
Plasmid: pAc-*tim*(S1404A)-HA	This paper	N/A
Plasmid: pAc-*tim*(S1404D)-HA	This paper	N/A
Plasmid: pMT-*ck2α*-V5	This paper	N/A
Plasmid: pMT-*ck2α*(Tik)-V5	This paper	N/A
Plasmid: pMT-V5	Thermo Fisher	Cat#V412020
Plasmid: pFastBac1-6XHIS	[88]	N/A
Plasmid: pFastBac1-6XHIS-d*clk*(1-1770)	This paper	N/A
Plasmid: pBA-*dpper*-FLAG	[84]	N/A
Plasmid: pHis::Parallel1	[89]	N/A
Software and Algorithms		
Fiji ImageJ (used for analysis of immunofluorescence microscopy images)	NIH Image	https://fiji.sc
GraphPad Prism 8 for Mac OS X	GraphPad Software	https://graphpad.com
FaasX	Laboratory of F. Rouyer; https://neuropsi.cnrs.fr/en/cnn-home/francois-rouyer/faasx-software/#thematique	Kit version: 1.22
Excel	Microsoft	Version 16.41